ACE2 diversity in placental mammals reveals the evolutionary strategy of SARS-C

Journal:	*Genetics and Molecular Biology*
Manuscript ID	Draft
Manuscript Type:	Original Article
Date Submitted by the Author:	n/a
Complete List of Authors:	Fam, Bibiana; UFRGS Instituto de Biociencias, Departamento de Genética Vargas-Pinilla, Pedro; Universidade de Sao Paulo, Depto de Bioquímica e Imunologia; Universidade Federal do Rio Grande do Sul, PPGBM Amorim, Eduardo; University of Lausanne, Department of Computational Biology Sortica, Vinicius; UFRGS Instituto de Biociencias, Departamento de Genética Bortolini, Maria Catira; UFRGS Instituto de Biociencias, Departamento de Genética
Keyword:	ACE2, placental mammals, SARS-CoV-2, COVID-19, inter and intra-species diversity

ACE2 diversity in placental mammals reveals the evolutionary strategy of SARS-Cov-2

Fam, BSO[1], Vargas-Pinilla, P[2], Amorim, CEG[3], Sortica, VA[1]*, and Bortolini[1], MC[1]*

Bibiana Sampaio de Oliveira Fam ORCID https://orcid.org/0000-0002-6654-6415

Pedro Vargas-Pinilla ORCID https://orcid.org/0000-0003-4622-0941

Carlos Eduardo G. Amorim ORCID https://orcid.org/0000-0002-8827-238X

Vinícius Albuquerque Sortica ORCID https://orcid.org/0000-0001-6185-0832

Maria Cátira Bortolini ORCID https://orcid.org/0000-0003-0598-3854

[1] Departamento de Genética, Instituto de Biociências, Universidade Federal do Rio Grande do Sul, Caixa Postal 15053, 91501-970 Porto Alegre, RS, Brazil;

[2] Departamento de Bioquímica e Imunologia, Faculdade de Medicina, Universidade de São Paulo, 14040-900 Ribeirão Preto, SP, Brazil;

[3]Department of Computational Biology, University of Lausanne,CH-

1015 Lausanne, Switzerland.

*Corresponding authors: Maria Cátira Bortolini and Vinícius A. Sortica (e-mails: maria.bortolini@ufrgs.br; vsortica@hotmail.com)

ABSTRACT The recent emergence of SARS-CoV-2 is responsible for the current pandemic of COVID-19, which uses the human membrane protein ACE2 as a gateway to the host-cell infection. We perform comparative genomic analysis of 70 ACE2 placental mammal orthologues to identify variations and contribute to the understanding of evolutionary dynamics behind this successful adaptation to infect humans. Our results reveal that 4% of the ACE2 sites are under positive selection, all located in the catalytic domain, suggesting possibly taxon-specific adaptations related to the ACE2 function, such as cardiovascular physiology. Considering all variable sites, we selected 30 of them located at the critical ACE2 binding sites to the SARS-CoV-like viruses to analyze in more detail. Our results reveal a relatively high diversity of ACE2 between placental mammal species while showing no polymorphism within human populations, at least considering the 30 inter-species variable sites. A perfect scenario for natural selection favored this opportunistic new coronavirus in its trajectory of infecting humans. We suggest that SARS-CoV-2 is a "generalist" coronavirus for human hosts, but not for other species. Differences in the rate of infection and mortality could be related to the innate immune responses, other unknown genetic factors, as well as non-biological factors.

KEY WORDS:

ACE2, placental mammals, SARS-CoV-2, COVID-19, inter and intra-species diversity

INTRODUCTION

The novel coronavirus SARS-CoV-2 (denominated before as 2019-nCOV) is a single-stranded RNA virus member of the Coronaviridae family. The estimates of the most recent common ancestor (MRCA) for the four coronavirus genera of this family range from 10,000 to millions of years (Wertheim *et al*, 2013). The most commented member of the Coronaviridae family at the moment, SARS-CoV-2, has a very recent origin. Based on genome sequence from different SARS-CoV-2 strains and a yearly mutation rate of 1.24 x 10^{-3} per site, Li *et al*. (2020a) estimated that it originated on November 24 2019.

SARS-CoV-2 is responsible for the current pandemic of Corona Virus Disease 2019 (COVID-19) (Chan *et al*., 2020; Huang *et al*., 2020; Wang *et al*., 2020; Coronaviridae Study Group, 2020). The COVID-19 was first reported in Wuhan (China) in December 2019 and spread worldwide, with a high rate of transmission, thousands of infected patients and many deaths between December 2019 and April 2020, and these numbers continue to grow. On March 11, WHO characterized COVID-19 as a pandemic, the first one caused by a coronavirus (WHO, situation report, March 11, 2020).SARS-CoV-2 cause a severe respiratory syndrome in humans, being transmitted arguably through different routes (*i.e.*, fomites, airborne or fecal-oral) by an animal to human and human to humans (Huang *et al.*, 2020; Li *et al.*, 2020b; Chan *et al.*, 2020), similar to SARS-CoV (Severe Acute Respiratory Syndrome-related coronavirus) and MERS-CoV (Middle East Respiratory Syndrome-related coronavirus). SARS-CoV was initially transmitted to humans from the palm civet (*Paguma larvata*; Kan *et al.*, 2005) and MERS-CoV by the dromedary (*Camelus dromedarius*; Zaki*et al.*, 2012). SARS-CoV-2 is classified as *Beta coronavirus* subgenus *Sar becovirus* with ~70% of similarity with SARS-CoV (Wu *et al.*, 2020). Genetic studies from different research groups found that SARS-CoV-2 is highly similar to the bat (*Rhinolophs affinis*) coronavirus (Li *et al.*, 2020b; Zhou *et al.*, 2020; Wu *et al.*, 2020; Ji *et al.*, 2020; Guo *et al.*, 2020). Other studies comparing genomes of different coronaviruses showed similarities between the human coronavirus and those from snakes, turtles, pangolins, and minks, suggesting these animals as possible intermediate-hosts (Wu *et al.*, 2020; Ji *et al.*, 2020; Guo *et al.*, 2020; Li *et al.*, 2020c, Liu *et al.*, 2020; Wan *et al.*, 2020). The most recent metagenomic study on the topic reinforces the idea that pangolins (*Manis javanica*) should be considered as the most plausible intermediate-host of SARS-CoV-2 related viruses, and that they acquired these viruses independently from bats or another animal hosts (Lam *et al.*, 2020). The authors found putative recombination signals between the pangolins coronaviruses, bat coronaviruses, and human SARS-CoV-2 (Lam *et al.*, 2020), which highlights the complexity of the origin of the new human coronavirus. Although there are uncertainties about the original and intermediate hosts, mutation and/or recombination among coronaviruses may have enabled cross-species infection (Letko*et al.*, 2020, Wan *et al.*, 2020).

Similar to SARS-CoV, SARS-CoV-2 utilizes the Angiotensin-Converting Enzyme 2 (ACE2) as receptor bind to infect cells (Li *et al.*, 2003; Li *et al.*, 2005a; Li *et al.*, 2005b Xu *et a*l., 2020; Letko *et al.*, 2020; Wan *et al.*, Chen et a.l, 2020; Li *et al.*, 2020a, Li *et al.*, 2020b, Hoffmann *et al.*, 2020; Walls *et al.*, 2020; Luan *et al.*, 2020). *ACE2* gene is located at chromosome X, and its product ACE2, a zinc metallopeptidase protein, comprises 805 amino acids containing a single catalytic domain. ACE2 is mainly expressed at vascular endothelium, myocardium, lungs, kidneys, and intestine (Turner *et al.*, 2004; McKinney *et al.*, 2014; Zhang *et al.*, 2020). It is a strict carboxypeptidase that hydrolyzes its substrate removing a single amino acid from their respective C-terminal. It is responsible for cleavage Angiotensin I and II into peptides Angiotensin 1-9 and Angiotensin 1-7, respectively, both are key elements connected with cardiovascular physiology, regulation of vascular tonus, blood pressure, electrolyte balance, and water intake (Millan *et al.*, 1990; Donoghue *et al.*, 2000; Oudit *et al.,* 2003; McKinney *et al.*, 2014).

ACE2 is a cell-surface non-raft protein with little intracellular localization, when binding to coronaviruses, the protein internalizes down-regulating activity from the cell surface (Hamming *et al.*, 2007). After SARS-CoV-like viruses and ACE2 attach, molecular cascade signal events result in entry of the coronavirus into the host cell (Simmons *et al.*, 2013), showing a successful evolutionary infection strategy. Kuba *et al.* (2005) showed that ACE2 down regulation mediated by SARS-CoV contributes to the acute lung injury, the most important clinical implication of human respiratory diseases caused by a coronavirus.

The success of a zoonotic spillover (transmission of a pathogen from a vertebrate animal to a human) is a complex process. It depends on several cultural, ecological, and climatic conditions, as well as features of viruses and hosts(Olival*et al.,* 2017). The efficiency in recognizing the host binding receptor is a crucial step, which defines the preference of the virus for a given species, tissue or cell type. The interaction of SARS-CoV-2 spike (S) glycoprotein, through its receptor-binding domain (RBD), happens via an optimized binding to human ACE2 domains (Andersen *et al.,* 2020; Hoffman *et al*., 2020; Walls *et al*., 2020). According to recent studies, five amino acid changes associated with natural selection in the critical binding sites (L455, F486, Q493, S494, N501) located at the SARS-CoV-2 S glycoprotein would be responsible for this high tropism with human ACE2 (Wan *et al*., 2020; Andersen *et al*., 2020). Furthermore, S glycoprotein of SARS-CoV-2 contains a cleavage site for furin proteases at the junction of subunits S1 and S2 (Coutard *et al*., 2020). During viral infection, S glycoprotein needs to be cleaved by host-cell proteases into S1 (which contains RBD) and S2 subunits. After this cleavage, the exposition of the S2 mediates fusion of the viral and host-cell membranes (Yan *et al*., 2020). Furin proteases are abundant in the respiratory tract, and this characteristic of the SARS-CoV-2 has been considered to be essential for successful infection of SARS-CoV-2 in human cells (Lam *et al.,* 2020). In contrast, the highly related bat and pangolin SARS-CoV-2-like coronavirus do not have the furin cleavage site, which in principle could be a barrier to zoonotic coronavirus spillover. Moreover, in SARS-CoV, furin-mediated cleavage of the S glycoprotein appears not to occur naturally (Simmons *et al.*, 2004) and the introduction of a functional furin cleavage site in the S1/S2 junction of SARS-CoV S glycoprotein resulted in a dramatic enhancement of cell-cell fusion (Follis and Nunberg, 2004).

Changes in key amino acids (AA) related to an efficient interaction between SARS-CoV-like S glycoprotein and ACE2 are crucial to cross-species infection, multi-host infections, as well as differences in susceptibility to disease and its symptoms in animal species. The evolutionary phenomena can be evoked to explain at least part of these events and conditions. To contribute to a better understanding of this complex process, we performed a comparative genomic analysis of 70 ACE2 orthologues, representative of placental mammal species, including pangolin, civet, bat, mink, and five New World monkey (NWm) species (Parvorder Platyrrhini). Furthermore, we describe the genetic variation of key binding sites across human populations. Our immediate goal is to reveal the taxon-specific variability in ACE2 amino acid sequence, its possible influence in cross-species SARS-CoV-2 infection, potential hosts, and other related topics that can be important and very timely considering the world outbreak of COVID-19.

MATERIAL AND METHODS

Sequences

Coding sequences for *ACE2* gene for 70 placental mammals species were retrieved trough BLAST from Genbank (www.ncbi.nlm.nih.gov accessed at 20/02/2020). For these analyses we considered sixteen domestic and fifty four wild species including representatives of orders Carnivora (N = 9), Ungulata (N = 11), Chiroptera (N = 10), Primates (N = 22), Rodentia (N = 9), and others (Table S1). Sequences were aligned according to the MUSCLE algorithm (Edgar, R, 2004) in Aliview software (Larson, A., 2014).

To investigate the variation within *Homo sapiens*, we used the Ensembl database (www.ensembl.org; Hunt, S. *et al,* 2018) and the UNIPROT database (www.uniprot.org, The Uniprot Consortium, 2019). Both platforms used data from 1000 Genome Project.

Evolutionary Analysis

The consensus phylogeny of species, based on neutral molecular markers, was obtained from the Timetree server (www.timetree.org; Kumar *et al.*, 2017). This phylogeny is used as a reference by specialized literature following Meredith *et al.* (2011). To better understand evolutionary patterns that are acting on *ACE2,* we performed a Site Model (NsSite) test with *Codeml* package in PAML 4.9 software (Yang, 2007*),* which allows inter-specific phylogenetic comparison substitution rates in protein-coding genes. This test allows ω variation (ω = dN/dS, being dN the rate of non- synonymous substitutions and dS the rate of synonymous substitutions) across sites. It fits neutral (ω~o), selective constraint (ω < 0), or positive selection (ω>1) models to the observed levels of variation. To determine which evolutionary model best fit to analyzed data we performed the Likelihood Ratio Tests to check the statistical significance between different models (Yang, 1998), for this, we compare neutral model (M1) against the model that allows positive selection (M2a) with df = 2 (Yang, 2007). Bayes Empirical Bayes (BEB) was used to infer sites with a high probability of being under positive selection (Yang *et al.,* 2005). Furthermore, we classify amino acid variation found in placental mammals ACE2 coding sequences categorizing amino acid changes into four classes of chemical similarity accordingly Grantham score (Grantham, 1974): conservative (GS = ≤ 50), moderately conservative (GS = 51–100), moderately radical (GS = 101–150), and radical (≥151).

RESULTS

Our results reveal that the M2 model (NsSite; ω > 1), significantly fits to the placental mammal *ACE2* data better than the neutral model ($\omega 2 = 2.58680$, $p < 0.001$; Table S2). Considering this model, 4% of the *ACE2* sites are under positive selection, a value high enough to infer a non-neutral molecular evolution for this gene as whole, at least considering placental mammals. Note, however, that this evolutionary scenario is not homogeneous across the different domains of the ACE2 protein. A parallel analysis, Bayes Empirical Bayes (BEB), highlights 22 sites (24, 34, 91, 93, 212, 228, 231, 251, 255, 286, 301, 387, 559, 568, 607, 653, 657, 658, 671, 675, 689, and 732) Table S3; Figure 1) with a high probability (> 95%) of being under positive selection, all of them being in the active sites at the extracellular portion (residues 18-740), where the ACE2 catalytic domain is located. Of the remaining ACE2 sites, 69% are under functional constrain due to the negative selection ($\omega 0 = 0.10125$), while 27% are with selective relaxation ($\omega 1 = 1$). For instance, the signal peptide (1-17), transmembrane domain (741 -761), and cytoplasmatic domain (761-805; see $\omega 3$ column of the Table S4) are more conserved, showing little variation across species, none of them with positive selection signals (Tables S2 and S4).

We note that ACE2 is a critical element in the cascade of regulation of blood pressure and cardiovascular condition, among other functions, and that these AA changes with a significant signal of positive selection could be taxon-specific, related to particular phenotypes found in some of these diverse placental mammals.

After that first evolutionary analysis, we examine all variable sites found considering the 70 orthologues. However, we choose only the 30 variable sites with information that they are functional and/or involved in the interaction between host-ACE2 and SARS-CoV-like viruses (Towler *et al.*, 2003; Li *et al.*, 2005a, 2020; Wan *et al.*, 2020; Luan *et al.*, 2020). Figure 2 shows the AAs observed in 30 chosen variable sites across the ACE2 orthologues of 70 selected placental mammal species. Three of them (24, 34, and 559) are target sites for positive selection, according to BEB (Table S3). Noteworthy, our purpose here is not to report each variation observed in the 70 orthologues, but to point out some thought-provoking findings to support the discussion and the main conclusion of the present study. The topology of Figure 2 recovers the phylogenetic relationship between the major taxonomic groups investigated. For example, *Homo sapiens* and all great apes (family Hominoidea) share the same amino acids in the 30 positions, and only one divergence, at the positive selection site 559 (conservative AA change, R559K; GS = 26), from Hominoidea to the Cercopithecidae species.

Position 24, which is one of the three sites with high probability of being under positive selection, has eight different amino acids segregating across taxon. Li and colleagues (2005) showed that the amino acid change from Glutamine to Lysine at position 24 (Q24K), together with a change from Lysine to Glutamate at position 26 (K26E), slightly inhibits interactions with SARS-CoV S glycoprotein (Li *et al.*, 2005). *Rattus norvegicus* has this combination (24K and 26E), while mouse species (*Mus musculus*, *Mus caroli,* and *Mus pahari*) have an Asparagine (N) at the position 24. *Rattus norvegicus* ACE2 also has the combination of Asparagine (N), Phenylalanine (F), and Serine (S) at positions 82-84. According to Li *et al.* (2005), this combination in rats (*R. norvegicus*) inhibits the interaction between ACE2 and SARS-CoV S glycoprotein. In addition, a Histidine (H) at positions 353 of ACE2 in the murine species also could inhibit or reduce the efficiency of the interaction according to Wan *et al.* (2020). Our study shows that murine species' ACE2 have only 56% of identity with the human ACE2 regarding these 30 binding sites. This reinforces the idea that they cannot naturally bind to S glycoprotein of SARS-CoV-2. On the other hand, Glutamine (Q) and Lysine (K) at 24 and 26 ACE2 positions are found in humans and all primates, as well as in *Cavia porcellus* (Guinea-pig), a rodent used very often as an experimental animal. However, there are differences in other important binding sites, resulting in the identity between Guinea-pig ACE2 and the human ACE2, regarding these 30 binding sites, being just 70%.

Cat (*Felis catus*) and dog (*Canis lupus familiars*) are of special interest due to their condition of close relationship with humans. Their ACE2 orthologues present at 77% and 73%, respectively, of identity with human ACE2, regarding the 30 variable sites. Both species present identity with other species belonging to the Carnivora order, such as Leucine (L) at position 24. However, they also show differences from each other at positions 25, 34, 427, and 559, two of them are a target for positive selection (34 and 559; Table S3). Therefore, 50% of the differences between the ACE2 binding sites of cat and dog are related to the evolution of taxon-specific variants that may be connected with specific functions of the ACE2 protein in each of these two domesticated species.

Interestingly, the five NWm and Prossimian species show different patterns than other primates at position 82-84. They present a moderately conserved change at position 82

(M82T; GS = 81), which also represents a change in polarity. We note that, due to the wide range of species that present the amino acid Threonine in that position, Threonine is probably the ancestral allele, meaning that a non-synonymous mutation promoted the AA alteration Threonine (T) > Methionine (M) in the ancestral branches of the Catarrhini clade. However, the ancestor of the Platyrrhini maintained the ancestral allele T. At position 41, we also found the same amino acid in NWm and Prossimian species. The moderately conservative modification Y41H (GS = 83) represents changes in charge, once Histidine (H) is an acid AA. Another mutation at this same site (Y41A; GS = 112) implies a moderately radical change and polarity difference, since Tyrosine (Y) is a polar AA, while Alanine (A) is a non-polar AA. This type of alteration could prevent viral interaction, at least with SARS-CoV according Li *et al.* (2005). Based on the distribution of the AAs at position 41 of ACE2, it seems that both NWm and Prossimian clades shared the derived allele (H), also seen in the bat genus *Hipposideros* and *Myotis*, as well as in *Equus*, suggesting molecular convergence.

NWm ACE2 is also different from other Primates species due to two changes in the potential glycosylation sites at positions 432 and 546 (Towler *et al.*, 2004), where Arginine

(N) was replaced by Serine (S). The glycosylation was suggested by the presence of electron density at all Arginine-linked site of the ACE2 N-terminal domain, including 432 and 546 and the loss of glycosylation sites may have functional implications (Towler *et al.*, 2004). Studies with MERS-CoV and with its host-cell entry receptor, DPP4, indicated that mutations that knock out glycosylation sites present in mouse DPP4 blocked the binding with MERS-CoV RBD (Peck *et al.*, 2017). The last authors concluded that glycosylation in DPP4 orthologue sites are a substantial barrier to MERS-CoV infection, particularly when combined with taxon-specific changes (Peck *et al.,* 2017).

We also observed a Serine (S) at the positively selected site 559, which reduces or inhibits the interaction of SARS-CoV S glycoprotein with ACE2 (Li *et al.*, 2005). A Serine in that position is found not only in rodents but also in some species of carnivores that were already considered as possible original or intermediate hosts such as pangolin (*Manis javanica*). Pangolin ACE2 has ~85% of similarity with human ACE2 (Lam *et al.*, 2020), but only 66% considering just these 30 sites investigated here. In addition, a Serine at position 559 is also observed in the two species of the Mustelidae family, ferret (*Mustela putorius*) and sea otter (*Enhydra lutris*).

Finally, we also leveraged intra-specific variation of the *ACE2* gene using data from human populations available in the 1000 Genomes Project (accessed through Ensembl and UNIPROT platforms). This dataset revealed 660 missense variants, 260 synonymous variants, 14,352 intron variants, 67 5'UTR variants, and 268 3'UTR variants in the *ACE2* gene in humans. Many of these have been investigated in case-control or genome-wide association studies for cardiovascular diseases and other correlated conditions (see for instance Ji *et al.,* 2017). Regarding the 30 ACE2 binding sites selected to present study (Figure 2), only one of them, at position 26, has two alleles segregating (K and R; Minor Allele Frequency or MAF = 0.002; rs4646116). Although we do not have population data for the other species investigated here, we observed that there is no relevant polymorphism regarding the 30 sites that promote the interaction between host-ACE2 and SARS-CoV-like viruses in the most studied species of all (*Homo sapiens*). This finding reinforces the idea that the AAs presented in Figure 2 are taxon-specific, *i.e.*, characteristic of a species or a taxonomic group, where intra-specific variation is absent or negligible. Also, the AA conservation within *Homo sapiens* in these 30 sites indicates an instigating evolutionary constraint whose reason needs to be better studied. A search in the genome of the Neanderthal (*Homo neanderthalensis*) and in the specimen of Denisova indicates that both present the same AAs, in these 30 sites, as *Homo sapiens*.

This finding reinforces the idea that the AAs presented in Figure 2 are taxon-specific, *i.e.*, characteristic of a species or a taxonomic group,where intra-specific variation is absent or negligible. Also, the AA conservation within *Homo sapiens* in these 30 sites indicates an instigating evolutionary constraint whose reason needs to be better studied. A search in the genome of the Neanderthal (*Homo neanderthalensis*) and in the specimen of Denisova shows that both present the same AAs, in these 30 sites, as the *Homo sapiens* ACE2.

DISCUSSION

Species of the Coronaviridae family can infect a wide variety of animals and humans, causing severe respiratory, enteric, hepatic, and neurological diseases (Weiss and Leibowitz, 2011). In humans, coronavirus has always caused mainly respiratory tract infections and, for decades, were considered with little clinical and epidemiological importance until SARS-CoV and MERS-CoV outbreaks (Kuiken *et al*., 2003; Zaki *et al*.

2012). Today, SARS-Cov-2 is responsible for the COVID-19, a pandemic that has challenged governments and peoples of every country in the world. COVID-19 already killed more persons than diseases caused by SARS-CoV and MERS-CoV combined, emphasizing the importance of this pathology as a highly relevant public health concern (WHO; https://www.who.int/emergencies/diseases/novel-coronavirus-2019).

SARS-CoV-like viruses use ACE2 as their gateway to the host cell. Figure 2 illustrates the diversity of 70 ACE2 orthologues, considering 30 potential binding sites to the S glycoproteins of the SARS-CoV-like viruses. This fact opens up a wide range of possibilities for this type of coronavirus, whose rate of evolution is high, due to its high rates of mutation and recombination (Li *et al*., 2020a). These phenomena that generate variability in the RNA viruses explain why they change host more frequently and jump between distantly related species than other pathogens (Woolhouse *et al*., 2005a, b; Davies and Pedersen, 2008; Longdon *et al*., 2014). These facts would explain a predicted origin of SARS-CoV-2 from original and/or intermediate phylogenetically distant hosts (for instance, bat and pangolin; Li *et al*., 2020c; Zhou *et al*., 2020; Wu *et al*., 2020; Ji *et al.,* 2020; Guo *et al*., 2020; Lam *et al*., 2020).

It was also known that specific pathogen mutations are often required to enhance pathogen's fitness in a new host (Longdon *et al.,* 2014). This is exactly what happened for the emergence of SARS-CoV-2. Recent investigations suggest the jump across species that resulted in the emergence of SARS-CoV-2 in humans was mainly due to five amino acid changes in critical S glycoprotein binding sites. Besides that, the S glycoprotein of SARS-CoV-2 contains a cleavage site for furin proteases at the junction of subunits S1and S2, differently than what occurs with bat and pangolin SARS-CoV-2-like coronavirus, and SARS-CoV (Coutard *et al.*, 2020). These events are associated with the high and efficient tropism with human ACE2 (Lam *et al.*, 2020; Andersen *et al.,* 2020). Besides, no relevant polymorphism was identified in these 30 ACE2 binding sites considering human populations. *Homo sapiens* is a “homogeneous” primate species, at least in regards to the 30 ACE2 important binding sites, and has a large population (census size of ~7.5 billion individuals) currently living in virtually all habitable places on Earth, including regions with very high demographic density. In other words, we can suggest that the high and efficient tropism is extended to all human populations, in addition to demographic and cultural conditions linked to the host that facilitate contagion and dispersion of this opportunistic coronavirus.

Hosts and pathogens are always in an evolutionary arms race. Several investigations reveal that coronavirus evolved to recognize different host-receptors, while others explain the host's strategies to defend themselves. For example, Peng *et al.* (2017) showed that a hepatitis coronavirus (MHV) infection driving the evolution of a mouse receptor (mCEACAM1a). In this case this event represented an answer to the intense selective pressure from a lethal infection (Peng *et al.*, 2017). More specifically, MHV uses mCEACAM1a as its host-receptor. Changes in critical amino acid residues led to the emergence of a derived-allele (m*CEACAM1b*) that is much more deficient as MHV receptor. Consequently, mice homozygous for this derived-allele are highly resistant to death from MHV infections (Peng *et al.*, 2017).

The first scientific report on the use of ACE2 as a host-cell entry portal by a coronavirus involved SARS-CoV (Li *et al.*, 2003). If it happened before, either with humans or other species, there is no way to know. Despite that, it is a short time to expect any evolutionary "reaction" from the host with a relatively long life cycle, at least regarding human *ACE2, i.e.,* it is not expected to happen as reported in the study of Peng et al. (2017) and the mouse receptor.

Therefore, as a consequence of the very recent evolution of its Spike glycoprotein and gain of a cleavage site for furin proteases, as well as the homogeneity of critical ACE2 binding sites across human populations and other demographic and cultural factors already mentioned above, SARS-CoV-2 obtained a significant edge in the evolutionary arms race, and become a highly infectious and pathogenic coronavirus for humans.

However, it is very well known that subsequent cell entry, pathogens can be blocked by neutralizing host-antibodies, which appears to be occurring in SARS-CoV-2 infections in humans. According to the WHO the majority of humans infected by SARS-CoV-2 have mild symptoms or are asymptomatic, despite that they have the same AAs in the ACE2 binding sites as reported here. The mechanisms of how antibodies neutralize a coronavirus infection have already been published (Hofman*et al.*, 2004; Reguera *et al.*, 2012; Li *et al.*, 2020a), illustrating that an innate agile and integrate (like those in young individuals) host-immune system is the first weapon to block the infection of opportunistic coronaviruses. Eventual population variability in other genetic systems, which may also be involved in this heterogeneity of COVID-19 symptoms and outcome cannot be ruled out.

On the other hand, the differences in these 30 important ACE2 binding sites of interaction with SARS-CoV-like viruses observed between species and taxonomic groups is striking, probably impacting the SARS-Cov-2's ability to bind with ACE2 in some of these species. The SARS-CoV-2 capacity to infect other 42 mammalian species was recently predicted based on changes at positions 31, 35, 38, 82, and 353 in the ACE2 orthologues when compared with the human ACE2 (Luan *et al.*, 2020). The last authors suggested that 76% of the 42 mammal species investigated, including pets (dog, *Canis lupus familiaris*, and cat, *Felis catus*), horse (*Equus caballus*), cattle (*Bos taurus*), and sheep (*Ovis aries*), may bind to S protein of SARS-CoV-2. The idea of a “generalist’ coronavirus, capable of infecting other species of mammals (pig, ferret, cat, orangutan, monkey) had also been defended by other authors, despite of the differences in their correspondent ACE2 orthologues (Wan *et al.*, 2020).

Here, we have expanded the comparative analysis to more species and sites of interaction between ACE2 orthologues and SARS-CoV-like viruses. Our results show that ACE2 murine species have only 56% of identity with human ACE2, and have also several critical taxon-specific changes that explain the barrier to infection with SARS-CoV-2. For the other species and taxon investigated here, however, the ability to block (or not) the infection to SARS-CoV-2 via this receptor is not easy to predict. At the moment preliminary results indicates that a macaque (*Macaca mulatta*) inoculated with SARS-CoV-2 recapitulates moderate respiratory disease observed in the majority of human cases (Munster *et al.,* 2020). Note that *Macaca mulatta*, similar to other species of the family Cercopithecidae, has only one change (R559K) relative to human and other species of the family Hominidae (*Pan troglodytes, Pan paniscus* and *Gorilla gorilla;* Figure 2). We also found a set of AA changes in the ACE2 of NWm species, which can characterize different patterns of binding to SARS-CoV-2, making them potentially less susceptible to the infection than humans and great apes. Earlier, one *in vivo* study (Greenough *et al.,* 2005) demonstrated SARS-CoV infection outcome in *Callithrix sp*., however, the pattern of virus replication and the potential risk for infection in nature for this and other NWm species has never been demonstrated. Therefore, *Callithrix sp.* although it is a good model for MERS-CoV (McAuliffe *et al*., 2004; Van Doremalen and Munster, 2015), it has not been established as an animal model to SARS-CoV infection. Note that MERS-CoV uses another host-cell entry receptor, DPP4, rather than ACE2.

When more *in vitro* and *in vivo* functional studies are performed, we will know which is the minimum AA combination in the ACE2 binding sites, and in other critical regions of the receptor, indispensable for an active connection with SARS-CoV-2 S glycoprotein. Until then, the predictions are speculative, but they can bring subsidies for future studies and strategies to contain the infection and its harmful consequences. Here we suggest that there are not many ACE2 orthologues with tropism for SARS-CoV-2, precisely because of its ability, shaped by natural selection, to use *Homo sapiens* ACE2 as an efficient and successful gateway to the host-cell. To our knowledge, there is only one preliminary *in vivo* study to test the susceptibility of animals to SARS-CoV-2 (Shi et al., 2020). The last authors intranasally inoculated ferrets, cats, dogs, pigs, chickens, and ducks with a dosage of SARS-CoV-2, and euthanized them some days post inoculation. They related that ferrets and cats are highly susceptible to SARS-CoV-2, dogs have low susceptibility, and livestock including pigs, chickens, and ducks are not susceptible to the SARS-CoV-2. On the other hand, there are no scientific record up to date of natural infection by SARS-CoV-2 in animals living in anthropogenic environments (only rare press reports, who described that cats, as well as tigers and lions from the New York Zoo were infected), an observation that challenges previous predictions that it would infect a wide range of species (Wan *et* *al.*, 2020; Luan *et al.*, 2020). The finding of absence from a veterinary epidemiological emergency during the current human COVID-19 pandemic, at least considering pets, also challenges the Shi et al.´s preliminary results, which indicated a high susceptible of cats to SARS-CoV-2 (Shi et al., 2020). If there is such a susceptibility to SARS-CoV-2 infection to these and other animals, it appears that it is much more restricted than that observed for humans.

It is also known that viruses that take advantage of receptors with conserved AA sequence have a broad host range (Woolhouse *et al.*, 2012). It is worth remembering again that ACE2 has conserved the AA sequence in crucial binding sites within *Homo sapiens*, but not between placental mammal species investigated here. In other words, the high mutation rate may provide alternatives to infect one of several species, but when a high tropism with the host cell is found, it can be predicted that the binding region has little (if any) variation within the species target.

Our findings reveal also that an essential part of this taxon-specific ACE2 diversity can even be attributed to the positive natural selection, since it is a membrane protein related to the water intake, blood pressure control, and other cardiovascular conditions. Besides that, a common trade-off of adapting to novel hosts is that performance on the original host is reduced (Longdon *et al.*, 2014). In other words, SARS-CoV-2 is a coronavirus with high performance to infect *Homo sapiens* individuals, from any population. In contrast, it could not infect, at least with the same efficiency, other species, as well as jump and re-infect the original or intermediate phylogenetically distant hosts (bats and/or pangolins). New mutations and/or recombination can turn SARS-CoV-2 into a derived-coronavirus capable of breaking down species barriers again, feeding the endless cycle of the arms race between host and pathogen.

On the other hand, closely related species may have similar levels of susceptibility, regardless of their distance from the pathogen's natural host (Longdon *et al.*, 2014). Then, due to the homology that ACE2 orthologues of the great apes have with the human ACE2 regarding the 30 binding sites investigated here, perhaps, only they are naturally and equally susceptible to develop symptoms of COVID-19, a concern that has already been demonstrated by members of the "Great Ape Health Consortium" (Gillespie and Leendertz, 2020).

CONCLUSION

Our comparative analysis of the ACE2 code region from 70 placental mammal species, revealed many variable sites. Of these, we selected 30 sites with records to be relevant for interaction with SARS-CoV-like S glycoproteins. For three of them, there is a significant sign of the action of the Darwinian (positive) selection. We observed extraordinary conservation within *Homo sapiens* and relatively high variation among placental mammal species. Our data indicate that SARS-CoV-2 has similar potential to infect any human population, already corroborated by the pandemic character of COVID-19. We can suggest that any difference in the rate of infection and mortality of this pathogen/disease among humans is related to other factors such as comorbidities of the infected individuals, cultural practices, demographic density, capacity of the country's health systems, suppression or mitigation measures, in addition to differences in the SARS-CoV-2 strains, as well as the effective innate immune response from infected individuals.The involvement of other genetic pathways, in addition to the ACE2 protein and the immune system, cannot be ruled out either, but only the progress of the studies will be able to identify them, as well as their eventual role in the COVID-19 human pandemic.

In conclusion, SARS-CoV-2 is highly “generalist” regarding its ability to infect humans, any human, at least considering its gateway to the cell, the ACE2 protein. In contrast, it is not a “generalist” coronavirus with the ability to infect, naturally and easily, a range of other species, including pets.

ACKNOWLEDGMENTS

This research was financially supported by the "Coordenação de Aperfeiçoamento de Pessoal de Nível Superior (CAPES)", and the "Conselho Nacional de Desenvolvimento Científico e Tecnológico (CNPq)". The funders had no role in study design, data collection and analysis, decision to publish, or preparation of the manuscript.

The authors declare that there is no conflict of interest that could be understood as prejudicial to the present research.

REFERENCES

Andersen KG, Rambaut A, Lipkin WI, Holmes EC and Garry RF (2020) The proximal origin of SARS-CoV-2. Nat Med. doi:10.1038/s41591-020-0820-9

Chan JF-W, Yuan S, Kok K-H, To KK-W, Chu H, Yang J, Xing F, Liu J, Yip CC-Y, Poon RW-S et al. (2020) A familial cluster of pneumonia associated with the 2019 novel coronavirus indicating person-to-person transmission: a study of a family cluster. The Lancet 395:514–523.doi:10.1016/S0140-6736(20)30154-9

Chen Y, Guo Y, Pan Y and Zhao ZJ (2020) Structure analysis of the receptor binding of 2019-nCoV. BiochemBiophys Res Commun.doi:10.1016/j.bbrc.2020.02.071

Coronaviridae Study Group of the International Committee on Taxonomy of Viruses (2020) The species Severe acute respiratory syndrome-related coronavirus: classifying 2019-nCoV and naming it SARS-CoV-2. Nat Microbiol 5:536–544.doi:10.1038/s41564-020-0695-z

Coutard B, Valle C, de Lamballerie X, Canard B, Seidah NG and Decroly E (2020) The spike glycoprotein of the new coronavirus 2019-nCoV contains a furin-like cleavage site absent in CoV of the same clade. Antiviral Research 176:104742. doi:10.1016/j.antiviral.2020.104742

Davies TJ and Pedersen AB (2008) Phylogeny and geography predict pathogen community similarity in wild primates and humans. ProcBiolSci 275:1695–1701.doi:10.1098/rspb.2008.0284

Follis KE, York J and Nunberg JH (2006) Furin cleavage of the SARS coronavirus spike glycoprotein enhances cell-cell fusion but does not affect virion entry. Virology 350:358–369.doi:10.1016/j.virol.2006.02.003

Gillespie TR and Leendertz FH (2020) COVID-19: protect great apes during human pandemics. Nature 579:497–497.doi:10.1038/d41586-020-00859-y

Grantham R (1974) Amino acid difference formula to help explain protein evolution. Science 185:862–864.doi:10.1126/science.185.4154.862

Greenough TC, Carville A, Coderre J, Somasundaran M, Sullivan JL, Luzuriaga K and Mansfield K (2005) Pneumonitis and Multi-Organ System Disease in Common Marmosets (*Callithrix jacchus*) Infected with the Severe Acute Respiratory Syndrome-Associated Coronavirus. The American Journal of Pathology 167:455–463.doi:10.1016/S0002-9440(10)62989-6

Guo Q, Li M, Wang C, Wang P, Fang Z, Tan J, Wu S, Xiao Y and Zhu H (2020) Host and infectivity prediction of Wuhan 2019 novel coronavirus using deep learning algorithm. bioRxiv 2020.01.21.914044. doi:10.1101/2020.01.21.914044

Hamming I, Cooper M, Haagmans B, Hooper N, Korstanje R, Osterhaus A, Timens W, Turner A, Navis G and van Goor H (2007) The emerging role of ACE2 in physiology and disease. J Pathol 212:1–11.doi:10.1002/path.2162

Hoffmann M, Kleine-Weber H, Schroeder S, Krüger N, Herrler T, Erichsen S, Schiergens TS, Herrler G, Wu N-H, Nitsche A et al. (2020) SARS-CoV-2 Cell Entry Depends on ACE2 and TMPRSS2 and Is Blocked by a Clinically Proven Protease Inhibitor. Cell S0092867420302294. doi:10.1016/j.cell.2020.02.052

Huang C, Wang Y, Li X, Ren L, Zhao J, Hu Y, Zhang L, Fan G, Xu J, Gu X et al. (2020) Clinical features of patients infected with 2019 novel coronavirus in Wuhan, China. The Lancet 395:497–506.doi:10.1016/S0140-6736(20)30183-5

Hunt SE, McLaren W, Gil L, Thormann A, Schuilenburg H, Sheppard D, Parton A, Armean IM, Trevanion SJ, Flicek P et al. (2018) Ensembl variation resources. 2018:12.

Ji L-D, Li J-Y, Yao B-B, Cai X-B, Shen Q-J and Xu J (2017) Are genetic polymorphisms in the renin-angiotensin-aldosterone system associated with essential hypertension? Evidence from genome-wide association studies.J Hum Hypertens 31:695–698.doi:10.1038/jhh.2017.29

Ji W, Wang W, Zhao X, Zai J and Li X (2020) Cross-species transmission of the newly identified coronavirus 2019-nCoV. J Med Virol 92:433–440.doi:10.1002/jmv.25682

Kan B, Wang M, Jing H, Xu H, Jiang X, Yan M, Liang W, Zheng H, Wan K, Liu Q et al. (2005) Molecular evolution analysis and geographic investigation of severe acute respiratory syndrome coronavirus-like virus in palm civets at an animal market and on farms. J Virol 79:11892–11900.doi:10.1128/JVI.79.18.11892-11900.2005

Kuba K, Imai Y, Rao S, Gao H, Guo F, Guan B, Huan Y, Yang P, Zhang Y, Deng W et al. (2005) A crucial role of angiotensin converting enzyme 2 (ACE2) in SARS coronavirus–induced lung injury. Nat Med 11:875–879.doi:10.1038/nm1267

Kuiken T, Fouchier RA, Schutten M, Rimmelzwaan GF, van Amerongen G, van Riel D, Laman JD, de Jong T, van Doornum G, Lim W et al. (2003) Newly discovered coronavirus as the primary cause of severe acute respiratory syndrome. The Lancet 362:263–270.doi:10.1016/S0140-6736(03)13967-0

Kumar R, Singh VP and Baker KM (2008) The intracellular renin-angiotensin system: implications in cardiovascular remodeling: Current Opinion in Nephrology and Hypertension 17:168–173. doi:10.1097/MNH.0b013e3282f521a8

Lam TT-Y, Shum MH-H, Zhu H-C, Tong Y-G, Ni X-B, Liao Y-S, Wei W, Cheung WY-M, Li W-J, Li L-F et al. (2020) Identifying SARS-CoV-2 related coronaviruses in Malayan pangolins. Nature. doi:10.1038/s41586-020-2169-0

Larsson A (2014) AliView: a fast and lightweight alignment viewer and editor for large datasets. Bioinformatics 30:3276–3278.doi:10.1093/bioinformatics/btu531

Letko M, Marzi A and Munster V (2020) Functional assessment of cell entry and receptor usage for SARS-CoV-2 and other lineage B betacoronaviruses.Nature Microbiology 5:562–569.doi:10.1038/s41564-020-0688-y

Li F, Li, W, Farzan, Michael and Harrison, Stephen (2005) Structure of SARS Coronavirus Spike Receptor-Binding Domain Complexed with Receptor.Science 309:1864–1868.doi: 10.1126/science.1116480

Li G, Fan Y, Lai Y, Han T, Li Z, Zhou P, Pan P, Wang W, Hu D, Liu X et al. (2020a) Coronavirus infections and immune responses. J Med Virol 92:424–432.doi:10.1002/jmv.25685

Li R, Qiao S and Zhang G (2020b) Analysis of angiotensin-converting enzyme 2 (ACE2) from different species sheds some light on cross-species receptor usage of a novel coronavirus 2019-nCoV. Journal of Infection 80:469–496.doi:10.1016/j.jinf.2020.02.013

Li W, Moore MJ, Vasilieva N, Sui J, Wong SK, Berne MA, Somasundaran M, Sullivan JL, Luzuriaga K, Greenough TC et al. (2003) Angiotensin-converting enzyme 2 is a functional receptor for the SARS coronavirus. Nature 426:450–454.doi:10.1038/nature02145

Li W, Zhang C, Sui J, Kuhn JH, Moore MJ, Luo S, Wong S-K, Huang I-C, Xu K, Vasilieva N et al. (2005) Receptor and viral determinants of SARS-coronavirus adaptation to human ACE2. EMBO J 24:1634–1643.doi:10.1038/sj.emboj.7600640

Li X, Zai J, Zhao Q, Nie Q, Li Y, Foley BT and Chaillon A (2020c) Evolutionary history, potential intermediate animal host, and cross‐species analyses of SARS-CoV-2. J Med Virol jmv.25731.doi:10.1002/jmv.25731

Longdon B, Brockhurst MA, Russell CA, Welch JJ and Jiggins FM (2014) The Evolution and Genetics of Virus Host Shifts. PLOS Pathogens 10:e1004395.doi:10.1371/journal.ppat.1004395

Liu Z, Xiao X, Wei X, Li J, Yang J, Tan H, Zhu J, Zhang Q, Wu J and Liu L (2020) Composition and divergence of coronavirus spike proteins and host ACE2 receptors predict potential intermediate hosts of SARS-CoV-2. J Med Virol jmv.25726.doi:10.1002/jmv.25726

McAuliffe J, Vogel L, Roberts A, Fahle G, Fischer S, Shieh W-J, Butler E, Zaki S, St. Claire M, Murphy B et al. (2004) Replication of SARS coronavirus administered into the respiratory tract of African Green, rhesus and cynomolgus monkeys. Virology 330:8–15.doi:10.1016/j.virol.2004.09.030

McKinney CA, Fattah C, Loughrey CM, Milligan G and Nicklin SA (2014) Angiotensin-(1-7) and angiotensin-(1-9): function in cardiac and vascular remodelling. ClinSci 126:815–827.doi:10.1042/CS20130436

Meredith RW, Janecka JE, Gatesy J, Ryder OA, Fisher CA, Teeling EC, Goodbla A, Eizirik E, Simao TLL, Stadler T et al. (2011) Impacts of the Cretaceous Terrestrial Revolution and KPg Extinction on Mammal Diversification. Science 334:521–524.doi:10.1126/science.1211028

Millan MA, Jacobowitz DM, Catt KJ and Aguilera G (1990) Distribution of angiotensin II receptors in the brain of nonhuman primates.Peptides 11:243–253.doi:10.1016/0196-9781(90)90077-I

Munster VJ, Koopmans M, van Doremalen N, van Riel D and de Wit E (2020) A Novel Coronavirus Emerging in China — Key Questions for Impact Assessment. New England Journal of Medicine 382:692–694.doi:10.1056/NEJMp2000929

Olival KJ, Hosseini PR, Zambrana-Torrelio C, Ross N, Bogich TL and Daszak P (2017) Host and viral traits predict zoonotic spillover from mammals. Nature 546:646–650.doi:10.1038/nature22975

Oudit GY, Kassiri Z, Jiang C, Liu PP, Poutanen SM, Penninger JM and Butany J (2009) SARS-coronavirus modulation of myocardial ACE2 expression and inflammation in patients with SARS. Eur J Clin Invest 39:618–625.doi:10.1111/j.1365-2362.2009.02153.x

Peck KM, Scobey T, Swanstrom J, Jensen KL, Burch CL, Baric RS and Heise MT (2017) Permissivity of Dipeptidyl Peptidase 4 Orthologs to Middle East Respiratory Syndrome Coronavirus Is Governed by Glycosylation and Other Complex Determinants. Journal of Virology.doi:10.1128/JVI.00534-17

Peng G, Yang Y, Pasquarella JR, Xu L, Qian Z, Holmes KV and Li F (2017) Structural and Molecular Evidence Suggesting Coronavirus-driven Evolution of Mouse Receptor. J BiolChem 292:2174–2181.doi:10.1074/jbc.M116.764266

Reguera J, Santiago C, Mudgal G, Ordoño D, Enjuanes L and Casasnovas JM (2012) Structural Bases of Coronavirus Attachment to Host Aminopeptidase N and Its Inhibition by Neutralizing Antibodies.PLoS Pathogens 8:e1002859.doi:10.1371/journal.ppat.1002859

Edgar RC (2004) MUSCLE: multiple sequence alignment with high accuracy and high throughput. Nucleic Acids Research 32:1792–1797.doi:10.1093/nar/gkh340

Simmons G, Reeves JD, Rennekamp AJ, Amberg SM, Piefer AJ and Bates P (2004) Characterization of severe acute respiratory syndrome-associated coronavirus (SARS-CoV) spike glycoprotein-mediated viral entry. Proc Natl Acad Sci USA 101:4240–4245. doi:10.1073/pnas.0306446101

Simmons G, Zmora P, Gierer S, Heurich A and Pöhlmann S (2013) Proteolytic activation of the SARS-coronavirus spike protein: Cutting enzymes at the cutting edge of antiviral research. Antiviral Research 100:605–614.doi:10.1016/j.antiviral.2013.09.028

Shi J, Wen Z, Zhong G, Yang H, Wang C, Liu R, He X, Shuai L, Sun Z, Zhao Y, Liang L, Cui1 P, Wang J , Zhang X , Guan Y, Chen H, and Bu Z (2020) Susceptibility of ferrets, cats, dogs, and different domestic animals to SARS-coronavirus. Preprint at bioRxiv https://doi.org/10.1101/2020.03.30.015347

Towler P, Staker B, Prasad SG, Menon S, Tang J, Parsons T, Ryan D, Fisher M, Williams D, Dales NA et al. (2004) ACE2 X-Ray Structures Reveal a Large Hinge-bending Motion Important for Inhibitor Binding and Catalysis. J BiolChem 279:17996–18007.doi:10.1074/jbc.M311191200

UniProt: a worldwide hub of protein knowledge (2019) Nucleic Acids Res 47:D506–D515. doi:10.1093/nar/gky1049

Van Doremalen N and Munster VJ (2015) Animal models of Middle East respiratory syndrome coronavirus infection. Antiviral Research 122:28–38.doi:10.1016/j.antiviral.2015.07.005

Walls AC, Park Y-J, Tortorici MA, Wall A, McGuire AT and Veesler D (2020) Structure, Function, and Antigenicity of the SARS-CoV-2 Spike Glycoprotein. Cell. doi:10.1016/j.cell.2020.02.058

Wan Y, Shang J, Graham R, Baric RS and Li F (2020) Receptor Recognition by the Novel Coronavirus from Wuhan: an Analysis Based on Decade-Long Structural Studies of SARS Coronavirus. J Virol 94:e00127-20, /jvi/94/7/JVI.00127-20.atom.doi:10.1128/JVI.00127-20

Wang C, Horby PW, Hayden FG and Gao GF (2020) A novel coronavirus outbreak of global health concern. The Lancet 395:470–473.doi:10.1016/S0140-6736(20)30185-9

Weiss SR and Leibowitz JL (2011) Chapter 4 - Coronavirus Pathogenesis. In: Maramorosch K, Shatkin AJ and Murphy FA (eds) Advances in Virus Research. Academic Press, pp 85–164

WHO situation report. Coronavirus Disease 2019 (COVID-19) Situation Report – 48. https://www.who.int/docs/default-source/coronaviruse/situation-reports/20200308-sitrep-48-covid-19.pdf?sfvrsn=16f7ccef_4. PDF access march 2020.

Woolhouse M, Scott F, Hudson Z, Howey R and Chase-Topping M (2012) Human viruses: discovery and emergence. Philos Trans R SocLond, B, BiolSci 367:2864–2871. doi:10.1098/rstb.2011.0354

Woolhouse MEJ and Gowtage-Sequeria S (2005) Host Range and Emerging and Reemerging Pathogens. Emerg Infect Dis 11:1842–1847. doi:10.3201/eid1112.050997

Woolhouse MEJ, Haydon DT and Antia R (2005) Emerging pathogens: the epidemiology and evolution of species jumps. Trends in Ecology & Evolution 20:238–244.doi:10.1016/j.tree.2005.02.009

Wu A, Peng Y, Huang B, Ding X, Wang X, Niu P, Meng J, Zhu Z, Zhang Z, Wang J et al. (2020) Genome Composition and Divergence of the Novel Coronavirus (2019-nCoV) Originating in China. Cell Host & Microbe 27:325–328. doi:10.1016/j.chom.2020.02.001

Xu X, Chen P, Wang J, Feng J, Zhou H, Li X, Zhong W and Hao P (2020) Evolution of the novel coronavirus from the ongoing Wuhan outbreak and modeling of its spike protein for risk of human transmission. Sci China Life Sci 63:457–460.doi:10.1007/s11427-020-1637-5

Yan R, Zhang Y, Li Y, Xia L, Guo Y and Zhou Q (2020) Structural basis for the recognition of SARS-CoV-2 by full-length human ACE2. Science 367:1444–1448.doi:10.1126/science.abb2762

Yang Z (1998) Likelihood ratio tests for detecting positive selection and application to primate lysozyme evolution.MolBiolEvol 15:568–573.doi:10.1093/oxfordjournals.molbev.a025957

Yang Z (2007) PAML 4: Phylogenetic Analysis by Maximum Likelihood. Molecular Biology and Evolution 24:1586–1591. doi:10.1093/molbev/msm088

Yang Z, Wong WSW and Nielsen R (2005) Bayes empirical bayes inference of amino acid sites under positive selection. MolBiolEvol 22:1107–1118.doi:10.1093/molbev/msi097

Zaki AM, van Boheemen S, Bestebroer TM, Osterhaus ADME and Fouchier RAM (2012) Isolation of a novel coronavirus from a man with pneumonia in Saudi Arabia. N Engl J Med 367:1814–1820.doi:10.1056/NEJMoa1211721

Zhang H, Penninger JM, Li Y, Zhong N and Slutsky AS (2020) Angiotensin-converting enzyme 2 (ACE2) as a SARS-CoV-2 receptor: molecular mechanisms and potential therapeutic target. Intensive Care Med 46:586–590.doi:10.1007/s00134-020-05985-9

Zhou P, Yang X-L, Wang X-G, Hu B, Zhang L, Zhang W, Si H-R, Zhu Y, Li B, Huang C-L et al. (2020) A pneumonia outbreak associated with a new coronavirus of probable bat origin. Nature 579:270–273.doi:10.1038/s41586-020-2012-7

Figure Legends

Figure 1. Three-dimensional structure of the ACE2 catalytic domain in gray, with sites with a high probability of being under positive selection highlighted in green. SARS-CoV-2 Spike glycoprotein is represented in blue.

Figure 2. Figure 2. Crucial variable sites in placental mammalian ACE2 protein.

Supplementary Material:

Table S1. Placental mammal species analyzed.

Table S2. Evolutionary rates estimated considering 70 *ACE2* placental mammal orthologues.

Table S3. Bayesian Empirical Bayes (BEB) analysis indicating sites with high probability (> 95%) to be under positive selection

Table S4. Bayes Empirical Bayes (BEB). General results. Signal peptide (1-17),extracellular domain (residues 18-740), transmembrane domain (741 -761), and cytoplasmatic domain (761-805). See ω3 column.

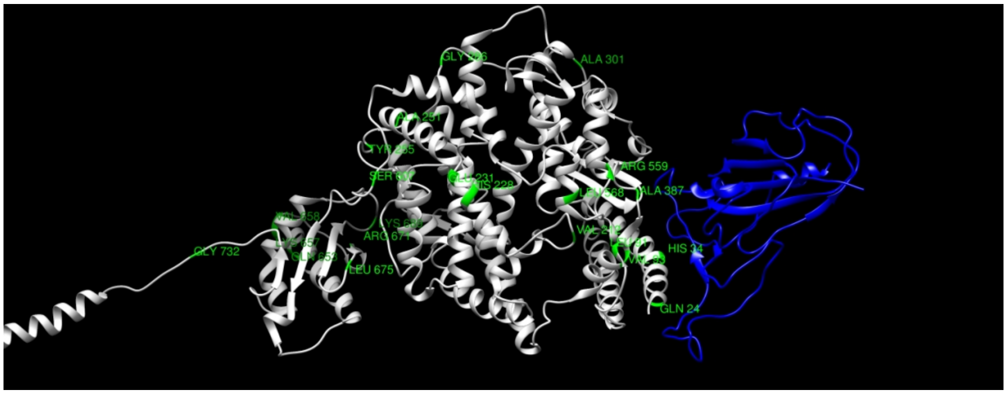

Figure 1. Three-dimensional structure of the ACE2 catalytic domain in gray, with sites with a high probability of being under positive selection highlighted in green. SARS-CoV-2 Spike glycoprotein is represented in blu

481x186mm (72 x 72 DPI)

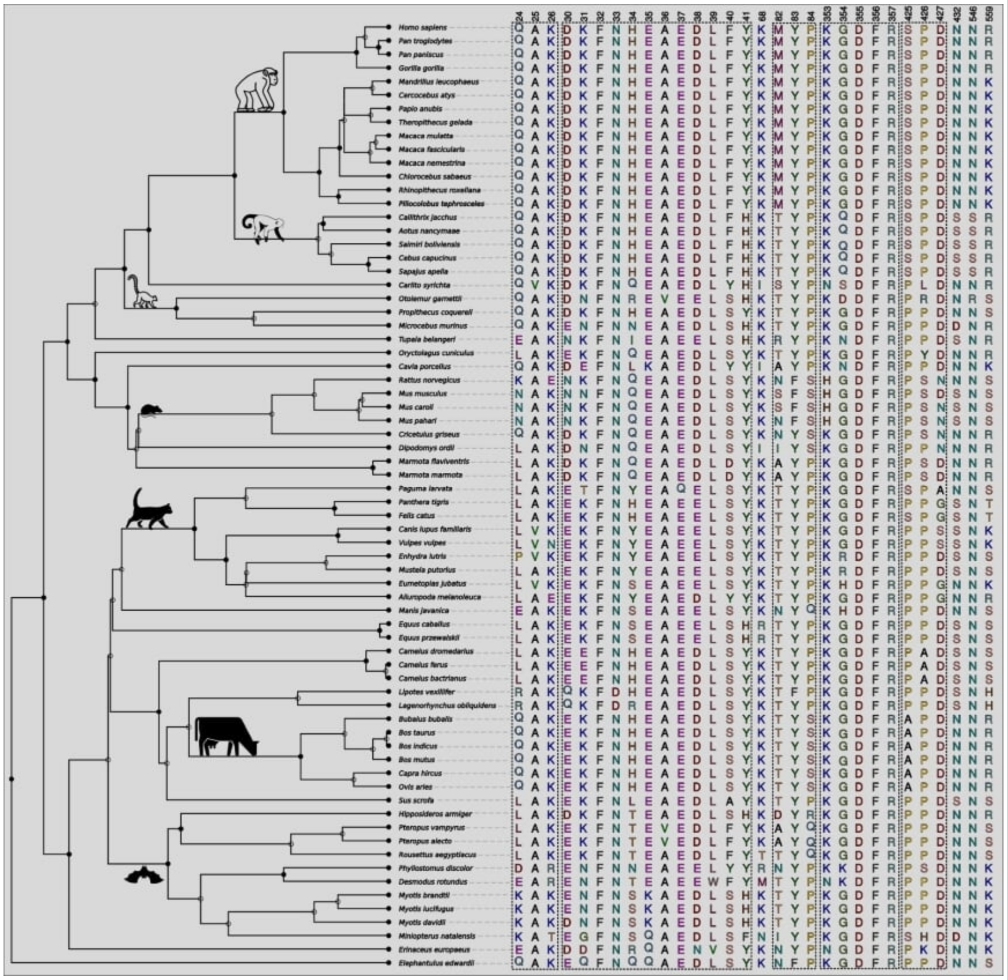

Figure 2. Figure 2. Crucial variable sites in placental mammalian ACE2 protein.

305x296mm (72 x 72 DPI)

Table S1. Placental mammal species analyzed.

ORDER	SPECIE	COMMON NAME	REFERENCE ACE2	Lenght
Carnivora	*Ailuropoda melanoleuca*	giant panda	XM_019793431.1	805
Carnivora	*Canis lupus familiaris*	dog	NM_001165260.1	804
Carnivora	*Enhydra lutris kenyoni*	sea otter	XM_022518370.1	805
Carnivora	*Eumetopias jubatus*	Steller sea lion	XM_028115021.1	806
Carnivora	*Felis catus*	domestic cat	XM_023248796.1	807
Carnivora	*Lagenorhynchus obliquidens*	Pacific white-sided dolphin	XM_027095797.1	804
Carnivora	*Mustela putorius furo*	domestic ferret	NM_001310190.1	805
Carnivora	*Paguma larvata*	Civet	AY881174.1	805
Carnivora	*Panthera tigris altaica*	Amur tiger	XM_007090080.2	797
Carnivora	*Vulpes vulpes*	red fox	XM_025986727.1	804
Cetartiodactyla	*Bos indicus*	zebu cattle	XM_019956161.1	804
Cetartiodactyla	*Bos mutus*	wild yak	XM_005903111.1	804
Cetartiodactyla	*Bos taurus*	cattle	XM_005228429.4	803
Cetartiodactyla	*Bubalus bubalis*	water buffalo	XM_006041540.2	803
Cetartiodactyla	*Camelus bactrianus*	Bactrian camel	XM_010968001.1	805
Cetartiodactyla	*Camelus dromedarius*	Arabian camel	XM_010993415.2	805
Cetartiodactyla	*Camelus ferus*	Wild Bactrian camel	XM_006194201.1	805
Cetartiodactyla	*Capra hircus*	goat	NM_001290107.1	804
Cetartiodactyla	*Lipotes vexillifer*	Yangtze River dolphin	XM_007466327.1	804

Cetartiodactyla	*Ovis aries*	sheep	XM_012106267.3	804
Cetartiodactyla	*Sus scrofa*	pig	NM_001123070.1	805
Chiroptera	*Desmodus rotundus*	common vampire bat	XM_024569930	804
Chiroptera	*Hipposideros armiger*	great roundleaf bat	XM_019667391.1	806
Chiroptera	*Miniopterus natalensis*	NA	XM_016202967.1	804
Chiroptera	*Myotis brandtii*	Brandts bat	XM_014544296.1	799
Chiroptera	*Myotis davidii*	NA	XM_015571433.1	799
Chiroptera	*Myotis lucifugus*	little brown bat	XM_023753671.1	799
Chiroptera	*Phyllostomus discolor*	pale spear-nosed bat	XM_028522516	804
Chiroptera	*Pteropus alecto*	black flying fox	XM_006911647.1	805
Chiroptera	*Pteropus vampyrus*	large flying fox	XM_011362973.2	804
Chiroptera	*Rousettus aegyptiacus*	Egyptian rousette	XM_016118926.1	805
Eulipotyphla	*Erinaceus europaeus*	western European hedgehog	XM_007538608.2	804
Lagomorpha	*Oryctolagus cuniculus*	rabbit	XM_002719845.3	805
Macroscelidea	*Elephantulus edwardii*	Cape elephant shrew	XM_006892395	798
Perissodactyla	*Equus caballus*	horse	XM_001490191.5	805
Perissodactyla	*Equus przewalskii*	Przewalskis horse	XM_008544773.1	805
Pholidota	*Manis javanica*	Malayan pangolin	XM_017650257.1	805
Primates	*Aotus nancymaae*	Mas night monkey	XM_012434682.2	805
Primates	*Callithrix jacchus*	white-tufted-ear marmoset	XM_008988993	805
Primates	*Carlito syrichta*	Philippine tarsier	XM_008064619	805
Primates	*Cebus capucinus imitator*	NA	XM_017512376	805

ORDER	SPECIE	COMMON NAME	REFERENCE ACE2	Lenght
Primates	*Cercocebus atys*	sooty mangabey	XM_012035808	805
Primates	*Chlorocebus sabaeus*	green monkey	XM_007991113	805
Primates	*Gorilla gorilla*	western gorilla	XM_019019204.1	805
Primates	*Homo sapiens*	human	NM_001371415.1	805
Primates	*Macaca fascicularis*	crab-eating macaque	XM_011545549	805
Primates	*Macaca mulatta*	Rhesus monkey	NM_001135696	805
Primates	*Macaca nemestrina*	pig-tailed macaque	XM_011735203	805
Primates	*Mandrillus leucophaeus*	drill	XM_011995533	805
Primates	*Microcebus murinus*	gray mouse lemur	XM_020285237.1	851
Primates	*Otolemur garnettii*	small-eared galago	XM_003791864.2	805
Primates	*Pan paniscus*	pygmy chimpanzee	XM_008974180.1	805
Primates	*Pan troglodytes*	chimpanzee	XM_016942979	805
Primates	*Papio anubis*	olive baboon	XM_021933040	805
Primates	*Piliocolobus tephrosceles*	Ugandan red Colobus	XM_023199053	805
Primates	*Propithecus coquereli*	Coquerels sifaka	XM_012638731.1	826
Primates	*Rhinopithecus roxellana*	golden snub-nosed monkey	XM_010366065	805
Primates	*Saimiri boliviensis*	Bolivian squirrel monkey	XM_010336623	805
Primates	*Sapajus apella*	Tufted capuchi	XM_032285963.1	805
Primates	*Theropithecus gelada*	gelada	XM_025372062	805
Rodentia	*Cavia porcellus*	domestic guinea pig	XM_023562040	813
Rodentia	*Cricetulus griseus*	Chinese hamster	XM_003503235	805

Rodentia	*Dipodomys ordii*	Ords kangaroo rat	XM_013032118	805
Rodentia	*Marmota flaviventris*	yellow-bellied marmot	XM_027946507	817
Rodentia	*Marmota marmota marmota*	Alpine marmot	XM_015488054	817
Rodentia	*Mus caroli*	Ryukyu mouse	XM_021153479	805
Rodentia	*Mus musculus*	house mouse	NM_027286	805
Rodentia	*Mus pahari*	shrew mouse	XM_021188276	805
Rodentia	*Rattus norvegicus*	Norway rat	NM_001012006	805
Scandentia	*Tupaia chinensis*	Chinese tree shrew	XM_006164692	805

Table S2. Evolutionary rates estimated considering 70 *ACE2* placental mammal orthologues.

Site Model	dN/dS	Estimated parameters	ℓ	*p*-value
M1: neutral	0,3658	p0= 0.70382, (p1= 0.29618) (ω0= 0.09888), (ω1= 1.00000)	-31476,87406	
M2a: selection	0,451	p0=0.68587, p1= 0.27167, (p2= 0.04246) (ω0= 0.10125), (ω1= 1.00000), ω2=2.58680	-31377,15314	$p<0{,}001$

p0= proportion of sites where $\omega < 1$; p1= proportion of sites where $\omega = 1$ and p2= proportion of sites where $\omega > 1$ (selection models only); $\omega 0 < 1$ (negative selection), $\omega 1 = 1$ (neutral selection) and $\omega 2 > 1$ (positive selection); Likelihood ratio tests were performed between neutral model (M1a), and model that identify positive selection (M2a). In the comparisons, M1a *vs* M2a has 2 degrees of freedom (df=2). Parentheses indicate fixed parameters.

Table S3. Bayesian Empirical Bayes (BEB) analysis indicating sites with high probability (> 95%) to be under positive selection.

Site	Probability of being under positive selection	Post mean +- SE for ω
24	0.985	2.231 +- 0.151
34	0.999	2.249 +- 0.040
91	1.000	2.250 +- 0.003
93	0.954	2.193 +- 0.262
212	1.000	2.249 +- 0.026
228	0.993	2.241 +- 0.105
231	0.994	2.243 +- 0.093
251	0.969	2.211 +- 0.218
255	0.985	2.232 +- 0.151
286	0.951	2.189 +- 0.269
301	0.999	2.248 +- 0.048
387	1.000	2.250 +- 0.011
559	0.990	2.237 +- 0.127
568	0.971	2.214 +- 0.209
607	0.987	2.234 +- 0.142
653	0.994	2.243 +- 0.095
657	0.998	2.248 +- 0.052
658	1.000	2.250 +- 0.005
671	1.000	2.250 +- 0.014
675	0.980	2.225 +- 0.175
689	0.999	2.249 +- 0.039
732	1.000	2.250 +- 0.008

Table S4. Bayes Empirical Bayes (BEB). General results. Signal peptide (1-17),extracellular domain (residues 18-740), transmembrane domain (741 -761), and cytoplasmatic domain (761-805). See ω3 column.

D	Site	W1	W2	W3	W	*D*	Site	W1	W2	W3	W
Signal peptide	1	1	0.00000	0.00000	0.10215		403	0.99995	0.00005	0.00000	0.10215
	2	0.02678	0.96877	0.00446	1		404	0.99864	0.00136	0.00000	0.10215
	3	0.03837	0.96139	0.00024	1		405	0.99988	0.00012	0.00000	0.10215
	4	0.99731	0.00269	0.00000	0.10215		406	0.99999	0.00001	0.00000	0.10215
	5	0.00000	0.78159	0.21841	1		407	0.99542	0.00458	0.00000	0.10215
	6	0.99489	0.00511	0.00000	0.10215		408	0.99999	0.00001	0.00000	0.10215
	7	0.99368	0.00632	0.00000	0.10215		409	0.99723	0.00277	0.00000	0.10215
	8	0.70401	0.29598	0.00001	0.10215		410	0.99977	0.00023	0.00000	0.10215
	9	0.99362	0.00638	0.00000	0.10215		411	0.99968	0.00032	0.00000	0.10215
	10	0.99948	0.00052	0.00000	0.10215		412	0.95922	0.04078	0.00000	0.10215
	11	0.98979	0.01021	0.00000	0.10215		413	0.99794	0.00206	0.00000	0.10215
	12	0.93414	0.06586	0.00000	0.10215		414	0.99986	0.00014	0.00000	0.10215
	13	0.98606	0.01394	0.00000	0.10215		415	0.99955	0.00045	0.00000	0.10215

	14	0.99896	0.00104	0.00000	0.10215		**416**	0.00010	0.99915	0.00075	1
	15	0.21743	0.78256	0.00001	1		**417**	0.99985	0.00015	0.00000	0.10215
	16	0.99818	0.00182	0.00000	0.10215		**418**	0.99752	0.00248	0.00000	0.10215
	17	0.99973	0.00027	0.00000	0.10215		**419**	0.99991	0.00009	0.00000	0.10215
	18	0.99603	0.00397	0.00000	0.10215		**420**	0.00000	0.66347	0.33653	1
	19	0.05376	0.94502	0.00122	1		**421**	0.96968	0.03032	0.00000	0.10215
	20	0.00008	0.98768	0.01224	1		**422**	0.99996	0.00004	0.00000	0.10215
	21	0.00000	0.98744	0.01255	1		**423**	0.99979	0.00021	0.00000	0.10215
	22	0.99993	0.00007	0.00000	0.10215		**424**	0.99679	0.00321	0.00000	0.10215
	23	0.97862	0.02138	0.00000	0.10215		**425**	0.33487	0.66492	0.00022	1
	24	0.00000	0.01801	0.98199	2,56612		**426**	0.00000	0.85601	0.14399	1
	25	0.65251	0.34747	0.00002	0.10215		**427**	0.95761	0.04239	0.00000	0.10215
	26	0.85409	0.14591	0.00000	0.10215		**428**	0.99995	0.00005	0.00000	0.10215
	27	0.00002	0.99209	0.00789	1		**429**	0.00000	0.49034	0.50966	2,56612
	28	0.99995	0.00005	0.00000	0.10215		**430**	0.99992	0.00008	0.00000	0.10215
	29	0.99796	0.00204	0.00000	0.10215		**431**	0.99999	0.00001	0.00000	0.10215
	30	0.00315	0.99680	0.00005	1		**432**	0.00095	0.99897	0.00009	1
	31	0.00001	0.99933	0.00066	1		**433**	0.99042	0.00958	0.00000	0.10215

	32	0.99995	0.00005	0.00000	0.10215		**434**	0.99986	0.00014	0.00000	0.10215
	33	0.99992	0.00008	0.00000	0.10215		**435**	0.05842	0.94156	0.00001	1
	34	0.00000	0.00105	0.99895	2,56612		**436**	0.99903	0.00097	0.00000	0.10215
	35	0.79593	0.20407	0.00000	0.10215		**437**	0.99999	0.00001	0.00000	0.10215
	36	0.99741	0.00259	0.00000	0.10215		**438**	0.99825	0.00175	0.00000	0.10215
	37	0.99999	0.00001	0.00000	0.10215		**439**	0.96557	0.03442	0.00001	0.10215
	38	0.49442	0.50558	0.00000	1		**440**	0.95944	0.04056	0.00000	0.10215
	39	0.83764	0.16227	0.00009	0.10215		**441**	0.99999	0.00001	0.00000	0.10215
	40	0.00002	0.98618	0.01380	1		**442**	0.99939	0.00061	0.00000	0.10215
	41	0.00081	0.99849	0.00070	1		**443**	0.99986	0.00014	0.00000	0.10215
	42	0.48810	0.51184	0.00006	1		**444**	0.99948	0.00052	0.00000	0.10215
	43	0.42642	0.57357	0.00000	1		**445**	0.78283	0.21717	0.00000	0.10215
	44	0.03240	0.96422	0.00338	1		**446**	0.99668	0.00332	0.00000	0.10215
	45	0.99976	0.00024	0.00000	0.10215		**447**	0.99724	0.00276	0.00000	0.10215
	46	0.99996	0.00004	0.00000	0.10215		**448**	0.99031	0.00969	0.00000	0.10215
	47	0.90859	0.09141	0.00000	0.10215		**449**	0.99965	0.00035	0.00000	0.10215
	48	0.99493	0.00507	0.00000	0.10215		**450**	0.96036	0.03963	0.00001	0.10215
	49	0.00197	0.99801	0.00002	1		**451**	0.99910	0.00090	0.00000	0.10215

	50	0.97093	0.02907	0.00000	0.10215		**452**	0.99993	0.00007	0.00000	0.10215
	51	0.99999	0.00001	0.00000	0.10215		**453**	0.99996	0.00004	0.00000	0.10215
	52	0.98944	0.01056	0.00000	0.10215		**454**	0.97632	0.02368	0.00000	0.10215
	53	1	0.00000	0.00000	0.10215		**455**	1	0.00000	0.00000	0.10215
	54	0.99999	0.00001	0.00000	0.10215		**456**	0.99703	0.00297	0.00000	0.10215
	55	0.99563	0.00437	0.00000	0.10215		**457**	0.99999	0.00001	0.00000	0.10215
	56	0.89717	0.10283	0.00000	0.10215		**458**	0.99999	0.00001	0.00000	0.10215
	57	0.99999	0.00001	0.00000	0.10215		**459**	0.96788	0.03211	0.00001	0.10215
	58	1	0.00000	0.00000	0.10215		**460**	0.99746	0.00254	0.00000	0.10215
	59	0.00000	0.78719	0.21281	1		**461**	0.96788	0.03211	0.00001	0.10215
	60	0.99594	0.00406	0.00000	0.10215		**462**	1	0.00000	0.00000	0.10215
	61	0.99620	0.00380	0.00000	0.10215		**463**	0.99979	0.00021	0.00000	0.10215
	62	1	0.00000	0.00000	0.10215		**464**	0.99994	0.00006	0.00000	0.10215
	63	0.99636	0.00364	0.00000	0.10215		**465**	0.00005	0.99926	0.00069	1
	64	0.00000	0.98659	0.01341	1		**466**	0.99976	0.00024	0.00000	0.10215
	65	0.97868	0.02132	0.00000	0.10215		**467**	0.97354	0.02646	0.00000	0.10215
	66	0.00001	0.99429	0.00570	1		**468**	0.99947	0.00053	0.00000	0.10215
	67	0.00000	0.94670	0.05330	1		**469**	0.99859	0.00141	0.00000	0.10215

	68	0.00405	0.99583	0.00012	1		**470**	0.96739	0.03261	0.00000	0.10215
	69	0.39636	0.60257	0.00107	1		**471**	0.51936	0.48064	0.00000	0.10215
	70	0.98528	0.01472	0.00000	0.10215		**472**	0.48085	0.51908	0.00007	1
	71	0.01717	0.98223	0.00060	1		**473**	0.99493	0.00507	0.00000	0.10215
	72	0.99995	0.00005	0.00000	0.10215		**474**	0.99597	0.00403	0.00000	0.10215
	73	0.99430	0.00570	0.00000	0.10215		**475**	0.00022	0.99932	0.00047	1
	74	0.99924	0.00076	0.00000	0.10215		**476**	0.99864	0.00136	0.00000	0.10215
	75	0.97003	0.02997	0.00000	0.10215		**477**	0.96676	0.03323	0.00001	0.10215
	76	0.46905	0.53088	0.00007	1		**478**	0.99493	0.00507	0.00000	0.10215
	77	0.69358	0.30634	0.00008	0.10215		**479**	0.99630	0.00370	0.00000	0.10215
	78	0.01012	0.98979	0.00009	1		**480**	1	0.00000	0.00000	0.10215
	79	0.00000	0.23458	0.76542	2,56612		**481**	0.99999	0.00001	0.00000	0.10215
	80	0.98752	0.01248	0.00000	0.10215		**482**	0.96682	0.03317	0.00001	0.10215
	81	0.21110	0.78888	0.00002	1		**483**	0.86425	0.13575	0.00000	0.10215
	82	0.00000	0.48804	0.51196	2,56612		**484**	0.99093	0.00907	0.00000	0.10215
	83	0.95644	0.04356	0.00000	0.10215		**485**	0.99994	0.00006	0.00000	0.10215
	84	0.05166	0.94705	0.00129	1		**486**	0.99989	0.00011	0.00000	0.10215
	85	0.40215	0.59682	0.00104	1		**487**	0.99991	0.00009	0.00000	0.10215

	86	0.00001	0.99120	0.00879	1		**488**	0.97435	0.02565	0.00000	0.10215
	87	0.00261	0.99732	0.00007	1		**489**	0.99999	0.00001	0.00000	0.10215
	88	0.99943	0.00057	0.00000	0.10215		**490**	0.99962	0.00038	0.00000	0.10215
	89	0.00269	0.99478	0.00252	1		**491**	0.00000	0.91016	0.08984	1
	90	0.08631	0.91368	0.00000	1		**492**	0.94910	0.05090	0.00000	0.10215
	91	0.00000	0.00001	0.99999	2,56612		**493**	0.99998	0.00002	0.00000	0.10215
	92	0.00000	0.95796	0.04204	1		**494**	0.99993	0.00007	0.00000	0.10215
	93	0.00000	0.14520	0.85480	2,56612		**495**	0.99999	0.00001	0.00000	0.10215
	94	0.99993	0.00007	0.00000	0.10215		**496**	0.99887	0.00113	0.00000	0.10215
	95	0.11417	0.88555	0.00027	1		**497**	0.99948	0.00052	0.00000	0.10215
	96	0.99937	0.00063	0.00000	0.10215		**498**	0.99973	0.00027	0.00000	0.10215
	97	0.99789	0.00211	0.00000	0.10215		**499**	0.99999	0.00001	0.00000	0.10215
	98	0.00002	0.97240	0.02758	1		**500**	0.99948	0.00052	0.00000	0.10215
	99	0.00000	0.80755	0.19245	1		**501**	0.99987	0.00013	0.00000	0.10215
	100	0.99958	0.00042	0.00000	0.10215		**502**	0.00002	0.98413	0.01586	1
	101	0.99632	0.00368	0.00000	0.10215		**503**	0.99675	0.00325	0.00000	0.10215
	102	0.00307	0.99494	0.00199	1		**504**	0.99825	0.00175	0.00000	0.10215
	103	0.80630	0.19370	0.00000	0.10215		**505**	0.99998	0.00002	0.00000	0.10215

	104	0.99910	0.00090	0.00000	0.10215		**506**	0.99997	0.00003	0.00000	0.10215
	105	0.75319	0.24677	0.00004	0.10215		**507**	0.98953	0.01047	0.00000	0.10215
	106	0.86360	0.13634	0.00006	0.10215		**508**	0.99992	0.00008	0.00000	0.10215
	107	0.00000	0.96295	0.03705	1		**509**	1	0.00000	0.00000	0.10215
	108	0.98734	0.01266	0.00000	0.10215		**510**	0.97830	0.02170	0.00000	0.10215
	109	0.55182	0.44786	0.00033	0.10215		**511**	0.99722	0.00278	0.00000	0.10215
	110	0.00003	0.99380	0.00617	1		**512**	0.99975	0.00025	0.00000	0.10215
	111	0.99683	0.00317	0.00000	0.10215		**513**	0.99994	0.00006	0.00000	0.10215
	112	0.99999	0.00001	0.00000	0.10215		**514**	0.99769	0.00231	0.00000	0.10215
	113	0.00000	0.94897	0.05103	1		**515**	0.99990	0.00010	0.00000	0.10215
	114	0.75270	0.24730	0.00000	0.10215		**516**	0.99683	0.00317	0.00000	0.10215
	115	0.00008	0.91865	0.08126	1		**517**	0.99986	0.00014	0.00000	0.10215
	116	0.99787	0.00213	0.00000	0.10215		**518**	0.99995	0.00005	0.00000	0.10215
	117	0.97646	0.02354	0.00000	0.10215		**519**	0.99974	0.00026	0.00000	0.10215
	118	0.00001	0.98492	0.01508	1		**520**	0.99991	0.00009	0.00000	0.10215
	119	0.99991	0.00009	0.00000	0.10215		**521**	0.99929	0.00071	0.00000	0.10215
	120	0.97939	0.02061	0.00000	0.10215		**522**	0.98065	0.01935	0.00000	0.10215
	121	0.22556	0.77444	0.00000	1		**523**	0.99976	0.00024	0.00000	0.10215

	122	0.00894	0.99069	0.00038	1		**524**	0.99944	0.00056	0.00000	0.10215
	123	1	0.00000	0.00000	0.10215		**525**	0.99995	0.00005	0.00000	0.10215
	124	0.99992	0.00008	0.00000	0.10215		**526**	0.88267	0.11732	0.00000	0.10215
	125	0.98902	0.01098	0.00000	0.10215		**527**	0.99999	0.00001	0.00000	0.10215
	126	0.97929	0.02071	0.00000	0.10215		**528**	0.99978	0.00022	0.00000	0.10215
	127	0.99950	0.00050	0.00000	0.10215		**529**	0.99978	0.00022	0.00000	0.10215
	128	0.99999	0.00001	0.00000	0.10215		**530**	0.99972	0.00028	0.00000	0.10215
	129	0.98847	0.01153	0.00000	0.10215		**531**	0.00000	0.73466	0.26534	1
	130	0.99982	0.00018	0.00000	0.10215		**532**	0.00031	0.99805	0.00164	1
	131	0.65821	0.34178	0.00000	0.10215		**533**	0.99996	0.00004	0.00000	0.10215
	132	0.99843	0.00157	0.00000	0.10215		**534**	0.29974	0.70025	0.00001	1
	133	0.98125	0.01875	0.00000	0.10215		**535**	0.99279	0.00721	0.00000	0.10215
	134	0.09024	0.90975	0.00001	1		**536**	0.82570	0.17430	0.00000	0.10215
	135	0.77391	0.22606	0.00003	0.10215		**537**	0.99992	0.00008	0.00000	0.10215
	136	0.00000	0.99839	0.00161	1		**538**	0.94632	0.05367	0.00000	0.10215
	137	0.91881	0.08119	0.00000	0.10215		**539**	0.99682	0.00318	0.00000	0.10215
	138	0.94983	0.05017	0.00000	0.10215		**540**	0.07295	0.92697	0.00008	1
	139	0.97344	0.02656	0.00000	0.10215		**541**	0.99935	0.00065	0.00000	0.10215

	140	0.99691	0.00309	0.00000	0.10215		**542**	0.99973	0.00027	0.00000	0.10215
	141	0.99893	0.00107	0.00000	0.10215		**543**	0.99999	0.00001	0.00000	0.10215
	142	0.00410	0.98413	0.01177	1		**544**	0.99992	0.00008	0.00000	0.10215
	143	0.00072	0.97069	0.02859	1		**545**	0.98225	0.01775	0.00000	0.10215
	144	0.99979	0.00021	0.00000	0.10215		**546**	0.99937	0.00063	0.00000	0.10215
	145	0.81519	0.18481	0.00000	0.10215		**547**	0.99885	0.00115	0.00000	0.10215
	146	0.99328	0.00672	0.00000	0.10215		**548**	0.00002	0.99535	0.00462	1
	147	0.99967	0.00033	0.00000	0.10215		**549**	0.99532	0.00468	0.00000	0.10215
	148	0.99801	0.00199	0.00000	0.10215		**550**	0.99996	0.00004	0.00000	0.10215
	149	0.96320	0.03680	0.00000	0.10215		**551**	0.99988	0.00012	0.00000	0.10215
	150	0.00000	0.77262	0.22738	1		**552**	0.00002	0.98876	0.01122	1
	151	0.99999	0.00001	0.00000	0.10215		**553**	0.99572	0.00428	0.00000	0.10215
	152	1	0.00000	0.00000	0.10215		**554**	0.99702	0.00298	0.00000	0.10215
	153	0.00055	0.99868	0.00078	1		**555**	0.39019	0.60966	0.00014	1
	154	0.00019	0.99919	0.00063	1		**556**	0.00000	0.96632	0.03368	1
	155	0.99994	0.00006	0.00000	0.10215		**557**	1	0.00000	0.00000	0.10215
	156	0.00051	0.99860	0.00090	1		**558**	0.97971	0.02028	0.00000	0.10215
	157	0.99999	0.00001	0.00000	0.10215		**559**	0.00000	0.01323	0.98677	2,56612

	158	0.99950	0.00050	0.00000	0.10215		**560**	0.99846	0.00154	0.00000	0.10215
	159	0.01040	0.98959	0.00001	1		**561**	0.99981	0.00019	0.00000	0.10215
	160	0.00000	0.44403	0.55597	2,56612		**562**	0.97028	0.02972	0.00000	0.10215
	161	0.99994	0.00006	0.00000	0.10215		**563**	0.99734	0.00266	0.00000	0.10215
	162	0.99904	0.00096	0.00000	0.10215		**564**	0.01951	0.98046	0.00003	1
	163	0.99493	0.00507	0.00000	0.10215		**565**	0.99856	0.00144	0.00000	0.10215
	164	0.91697	0.08303	0.00000	0.10215		**566**	0.99493	0.00507	0.00000	0.10215
	165	0.99493	0.00507	0.00000	0.10215		**567**	0.99976	0.00024	0.00000	0.10215
	166	0.99999	0.00001	0.00000	0.10215		**568**	0.00000	0.03607	0.96393	2,56612
	167	0.68776	0.31223	0.00001	0.10215		**569**	0.99987	0.00013	0.00000	0.10215
	168	0.99493	0.00507	0.00000	0.10215		**570**	0.99772	0.00228	0.00000	0.10215
	169	0.99993	0.00007	0.00000	0.10215		**571**	0.97598	0.02402	0.00000	0.10215
	170	0.00547	0.99384	0.00069	1		**572**	0.00000	0.96747	0.03253	1
	171	0.09281	0.90718	0.00001	1		**573**	0.00333	0.99632	0.00034	1
	172	0.99452	0.00548	0.00000	0.10215		**574**	0.99929	0.00071	0.00000	0.10215
	173	0.99975	0.00025	0.00000	0.10215		**575**	0.99110	0.00890	0.00000	0.10215
	174	0.99952	0.00048	0.00000	0.10215		**576**	0.00000	0.90879	0.09121	1
	175	0.99614	0.00386	0.00000	0.10215		**577**	0.76767	0.23233	0.00000	0.10215

	176	0.99667	0.00333	0.00000	0.10215		**578**	0.23779	0.76221	0.00000	1
	177	0.99995	0.00005	0.00000	0.10215		**579**	1	0.00000	0.00000	0.10215
	178	0.99911	0.00089	0.00000	0.10215		**580**	0.87200	0.12800	0.00000	0.10215
	179	0.39392	0.60514	0.00094	1		**581**	0.99449	0.00551	0.00000	0.10215
	180	0.99991	0.00009	0.00000	0.10215		**582**	0.00000	0.97716	0.02284	1
	181	0.99999	0.00001	0.00000	0.10215		**583**	0.99910	0.00090	0.00000	0.10215
	182	0.99999	0.00001	0.00000	0.10215		**584**	0.99692	0.00308	0.00000	0.10215
	183	0.99989	0.00011	0.00000	0.10215		**585**	0.99909	0.00091	0.00000	0.10215
	184	0.99991	0.00009	0.00000	0.10215		**586**	0.00960	0.99036	0.00004	1
	185	0.00009	0.99292	0.00699	1		**587**	0.99946	0.00054	0.00000	0.10215
	186	0.99699	0.00301	0.00000	0.10215		**588**	0.99994	0.00006	0.00000	0.10215
	187	0.99989	0.00011	0.00000	0.10215		**589**	0.97007	0.02993	0.00000	0.10215
	188	1	0.00000	0.00000	0.10215		**590**	0.99878	0.00122	0.00000	0.10215
	189	0.99999	0.00001	0.00000	0.10215		**591**	0.99806	0.00194	0.00000	0.10215
	190	1	0.00000	0.00000	0.10215		**592**	0.01817	0.98172	0.00011	1
	191	0.99986	0.00014	0.00000	0.10215		**593**	0.17323	0.82663	0.00015	1
	192	0.99635	0.00365	0.00000	0.10215		**594**	0.99493	0.00507	0.00000	0.10215
	193	0.94756	0.05244	0.00000	0.10215		**595**	0.99684	0.00316	0.00000	0.10215

	194	0.97887	0.02113	0.00000	0.10215		**596**	0.96260	0.03740	0.00000	0.10215
	195	0.01284	0.98715	0.00001	1		**597**	0.00000	0.97341	0.02659	1
	196	0.99989	0.00011	0.00000	0.10215		**598**	0.99622	0.00378	0.00000	0.10215
	197	0.97651	0.02349	0.00000	0.10215		**599**	0.99999	0.00001	0.00000	0.10215
	198	0.99999	0.00001	0.00000	0.10215		**600**	0.00001	0.99466	0.00534	1
	199	0.99988	0.00012	0.00000	0.10215		**601**	0.99959	0.00041	0.00000	0.10215
	200	0.99988	0.00012	0.00000	0.10215		**602**	0.99960	0.00040	0.00000	0.10215
	201	1	0.00000	0.00000	0.10215		**603**	0.01296	0.98685	0.00020	1
	202	0.99990	0.00010	0.00000	0.10215		**604**	0.99924	0.00076	0.00000	0.10215
	203	0.99493	0.00507	0.00000	0.10215		**605**	0.99984	0.00016	0.00000	0.10215
	204	0.99990	0.00010	0.00000	0.10215		**606**	0.99493	0.00507	0.00000	0.10215
	205	0.18546	0.81446	0.00009	1		**607**	0.00000	0.03786	0.96214	2,56612
	206	0.99991	0.00009	0.00000	0.10215		**608**	0.91508	0.08492	0.00000	0.10215
	207	0.99991	0.00009	0.00000	0.10215		**609**	0.00000	0.89093	0.10907	1
	208	0.99941	0.00059	0.00000	0.10215		**610**	0.96502	0.03497	0.00001	0.10215
	209	0.00227	0.99728	0.00045	1		**611**	0.24780	0.75219	0.00001	1
	210	0.44445	0.55555	0.00000	1		**612**	0.99313	0.00687	0.00000	0.10215
	211	0.84070	0.15930	0.00000	0.10215		**613**	0.35665	0.64333	0.00002	1

	212	0.00000	0.00037	0.99963	2,56612		**614**	0.00001	0.99573	0.00426	1
	213	0.00000	0.97287	0.02713	1		**615**	0.08606	0.91393	0.00001	1
	214	0.64828	0.35170	0.00001	0.10215		**616**	0.11184	0.88783	0.00033	1
	215	0.99031	0.00969	0.00000	0.10215		**617**	0.32536	0.67462	0.00002	1
	216	0.00000	0.81285	0.18715	1		**618**	0.99995	0.00005	0.00000	0.10215
	217	0.99909	0.00091	0.00000	0.10215		**619**	0.99999	0.00001	0.00000	0.10215
	218	0.00083	0.99879	0.00038	1		**620**	0.99991	0.00009	0.00000	0.10215
	219	0.26603	0.73359	0.00038	1		**621**	0.99994	0.00006	0.00000	0.10215
	220	0.00000	0.42366	0.57634	2,56612		**622**	0.99999	0.00001	0.00000	0.10215
	221	0.99637	0.00363	0.00000	0.10215		**623**	0.99992	0.00008	0.00000	0.10215
	222	0.99785	0.00215	0.00000	0.10215		**624**	0.99644	0.00356	0.00000	0.10215
	223	0.15425	0.84575	0.00000	1		**625**	0.99942	0.00058	0.00000	0.10215
	224	0.00000	0.99538	0.00462	1		**626**	0.15588	0.84245	0.00167	1
	225	0.99999	0.00001	0.00000	0.10215		**627**	0.99974	0.00026	0.00000	0.10215
	226	0.99910	0.00090	0.00000	0.10215		**628**	0.99981	0.00019	0.00000	0.10215
	227	0.99942	0.00058	0.00000	0.10215		**629**	0.99981	0.00019	0.00000	0.10215
	228	0.00000	0.02022	0.97978	2,56612		**630**	0.00000	0.29321	0.70679	2,56612
	229	0.04762	0.95216	0.00022	1		**631**	0.00000	0.97292	0.02708	1

	230	0.99993	0.00007	0.00000	0.10215		**632**	0.99379	0.00621	0.00000	0.10215
	231	0.00000	0.03886	0.96114	2,56612		**633**	0.99893	0.00107	0.00000	0.10215
	232	0.93838	0.06162	0.00000	0.10215		**634**	0.00005	0.99941	0.00053	1
	233	0.99938	0.00062	0.00000	0.10215		**635**	0.99493	0.00507	0.00000	0.10215
	234	0.99920	0.00080	0.00000	0.10215		**636**	0.99988	0.00012	0.00000	0.10215
	235	0.99906	0.00094	0.00000	0.10215		**637**	0.87508	0.12492	0.00000	0.10215
	236	0.99721	0.00279	0.00000	0.10215		**638**	0.99590	0.00410	0.00000	0.10215
	237	0.99990	0.00010	0.00000	0.10215		**639**	0.99999	0.00001	0.00000	0.10215
	238	0.97018	0.02982	0.00000	0.10215		**640**	0.99769	0.00231	0.00000	0.10215
	239	0.00007	0.99868	0.00125	1		**641**	0.97837	0.02163	0.00000	0.10215
	240	0.99977	0.00023	0.00000	0.10215		**642**	0.22111	0.77807	0.00083	1
	241	0.99998	0.00002	0.00000	0.10215		**643**	0.99974	0.00026	0.00000	0.10215
	242	0.99990	0.00010	0.00000	0.10215		**644**	0.00000	0.14533	0.85467	2,56612
	243	0.99934	0.00066	0.00000	0.10215		**645**	0.88881	0.11116	0.00003	0.10215
	244	0.99991	0.00009	0.00000	0.10215		**646**	0.88418	0.11582	0.00000	0.10215
	245	0.99994	0.00006	0.00000	0.10215		**647**	0.00103	0.99871	0.00026	1
	246	0.00000	0.72863	0.27137	1		**648**	0.99986	0.00014	0.00000	0.10215
	247	0.99999	0.00001	0.00000	0.10215		**649**	0.99929	0.00071	0.00000	0.10215

	248	0.99799	0.00201	0.00000	0.10215		**650**	0.98847	0.01153	0.00000	0.10215
	249	0.99999	0.00001	0.00000	0.10215		**651**	0.99996	0.00004	0.00000	0.10215
	250	0.00894	0.99104	0.00002	1		**652**	0.99991	0.00009	0.00000	0.10215
	251	0.00000	0.04017	0.95983	2,56612		**653**	0.00000	0.00671	0.99329	2,56612
	252	0.99953	0.00047	0.00000	0.10215		**654**	0.94393	0.05607	0.00000	0.10215
	253	0.99965	0.00035	0.00000	0.10215		**655**	0.99995	0.00005	0.00000	0.10215
	254	0.93674	0.06326	0.00001	0.10215		**656**	0.00000	0.31527	0.68473	2,56612
	255	0.00000	0.02186	0.97814	2,56612		**657**	0.00000	0.00190	0.99810	2,56612
	256	0.97447	0.02553	0.00000	0.10215		**658**	0.00000	0.00001	0.99999	2,56612
	257	0.97129	0.02871	0.00000	0.10215		**659**	0.99465	0.00535	0.00000	0.10215
	258	0.99915	0.00085	0.00000	0.10215		**660**	0.00000	0.99720	0.00279	1
	259	0.66603	0.33397	0.00000	0.10215		**661**	0.86992	0.13008	0.00001	0.10215
	260	0.99981	0.00019	0.00000	0.10215		**662**	0.00027	0.99806	0.00168	1
	261	0.73199	0.26797	0.00004	0.10215		**663**	0.00214	0.99778	0.00008	1
	262	0.99917	0.00083	0.00000	0.10215		**664**	0.00000	0.63367	0.36633	1
	263	0.99965	0.00035	0.00000	0.10215		**665**	0.99994	0.00006	0.00000	0.10215
	264	0.99991	0.00009	0.00000	0.10215		**666**	0.00014	0.99698	0.00288	1
	265	0.99998	0.00002	0.00000	0.10215		**667**	0.00000	0.92432	0.07568	1

	266	0.99803	0.00197	0.00000	0.10215		**668**	0.00005	0.99951	0.00044	1
	267	0.99977	0.00023	0.00000	0.10215		**669**	0.00117	0.99879	0.00004	1
	268	0.99995	0.00005	0.00000	0.10215		**670**	0.99934	0.00066	0.00000	0.10215
	269	1	0.00000	0.00000	0.10215		**671**	0.00000	0.00007	0.99993	2,56612
	270	1	0.00000	0.00000	0.10215		**672**	0.98943	0.01057	0.00000	0.10215
	271	0.99493	0.00507	0.00000	0.10215		**673**	0.00000	0.99226	0.00774	1
	272	0.99996	0.00004	0.00000	0.10215		**674**	0.84342	0.15658	0.00000	0.10215
	273	0.99990	0.00010	0.00000	0.10215		**675**	0.00000	0.02339	0.97661	2,56612
	274	0.99995	0.00005	0.00000	0.10215		**676**	0.77035	0.22965	0.00000	0.10215
	275	0.99493	0.00507	0.00000	0.10215		**677**	0.16823	0.83116	0.00061	1
	276	0.99914	0.00086	0.00000	0.10215		**678**	0.99989	0.00011	0.00000	0.10215
	277	0.99993	0.00007	0.00000	0.10215		**679**	0.00005	0.99695	0.00300	1
	278	0.99705	0.00295	0.00000	0.10215		**680**	0.99865	0.00135	0.00000	0.10215
	279	0.99949	0.00051	0.00000	0.10215		**681**	0.99977	0.00023	0.00000	0.10215
	280	0.00000	0.69098	0.30902	1		**682**	0.00002	0.99852	0.00146	1
	281	0.98543	0.01457	0.00000	0.10215		**683**	0.99974	0.00026	0.00000	0.10215
	282	0.67652	0.32347	0.00001	0.10215		**684**	0.00007	0.99846	0.00148	1
	283	0.47440	0.52559	0.00001	1		**685**	0.99980	0.00020	0.00000	0.10215

	284	0.99868	0.00132	0.00000	0.10215		**686**	0.99996	0.00004	0.00000	0.10215
	285	0.98226	0.01774	0.00000	0.10215		**687**	0.00000	0.39883	0.60117	2,56612
	286	0.00000	0.07530	0.92470	2,56612		**688**	0.99738	0.00262	0.00000	0.10215
	287	0.00058	0.99586	0.00356	1		**689**	0.00000	0.00203	0.99797	2,56612
	288	0.99991	0.00009	0.00000	0.10215		**690**	0.98714	0.01286	0.00000	0.10215
	289	0.99909	0.00091	0.00000	0.10215		**691**	0.00000	0.64629	0.35371	1
	290	0.99910	0.00090	0.00000	0.10215		**692**	0.17166	0.82822	0.00013	1
	291	0.99999	0.00001	0.00000	0.10215		**693**	0.00200	0.99791	0.00009	1
	292	1	0.00000	0.00000	0.10215		**694**	0.00005	0.99658	0.00338	1
	293	0.99980	0.00020	0.00000	0.10215		**695**	0.99613	0.00387	0.00000	0.10215
	294	0.99996	0.00004	0.00000	0.10215		**696**	0.99962	0.00038	0.00000	0.10215
	295	0.00022	0.99971	0.00007	1		**697**	0.99603	0.00397	0.00000	0.10215
	296	0.00029	0.99816	0.00155	1		**698**	0.00000	0.97188	0.02812	1
	297	1	0.00000	0.00000	0.10215		**699**	0.86554	0.13445	0.00000	0.10215
	298	0.00000	0.97958	0.02042	1		**700**	0.99997	0.00003	0.00000	0.10215
	299	0.00000	0.99742	0.00258	1		**701**	0.99999	0.00001	0.00000	0.10215
	300	0.99945	0.00055	0.00000	0.10215		**702**	0.00000	0.91995	0.08005	1
	301	0.00000	0.00313	0.99687	2,56612		**703**	0.99889	0.00111	0.00000	0.10215

	302	0.99493	0.00507	0.00000	0.10215		**704**	0.99622	0.00378	0.00000	0.10215
	303	0.52612	0.47388	0.00000	0.10215		**705**	0.60448	0.39552	0.00000	0.10215
	304	0.99907	0.00093	0.00000	0.10215		**706**	0.00000	0.99972	0.00028	1
	305	0.00000	0.36274	0.63726	2,56612		**707**	0.72928	0.27067	0.00005	0.10215
	306	0.58170	0.41830	0.00000	0.10215		**708**	0.99817	0.00183	0.00000	0.10215
	307	0.99999	0.00001	0.00000	0.10215		**709**	0.00000	0.92595	0.07405	1
	308	0.99848	0.00152	0.00000	0.10215		**710**	0.99949	0.00051	0.00000	0.10215
	309	0.00614	0.99377	0.00009	1		**711**	0.99992	0.00008	0.00000	0.10215
	310	0.99999	0.00001	0.00000	0.10215		**712**	1	0.00000	0.00000	0.10215
	311	0.99995	0.00005	0.00000	0.10215		**713**	0.99880	0.00120	0.00000	0.10215
	312	0.99999	0.00001	0.00000	0.10215		**714**	0.00001	0.99569	0.00430	1
	313	0.99705	0.00295	0.00000	0.10215		**715**	0.99982	0.00018	0.00000	0.10215
	314	0.99975	0.00025	0.00000	0.10215		**716**	0.00000	0.84575	0.15425	1
	315	0.99963	0.00037	0.00000	0.10215		**717**	0.99668	0.00332	0.00000	0.10215
	316	0.06299	0.93686	0.00015	1		**718**	0.99992	0.00008	0.00000	0.10215
	317	0.99786	0.00214	0.00000	0.10215		**719**	0.99999	0.00001	0.00000	0.10215
	318	0.93997	0.06003	0.00000	0.10215		**720**	0.99699	0.00301	0.00000	0.10215
	319	0.99166	0.00834	0.00000	0.10215		**721**	0.00140	0.99790	0.00070	1

	320	0.99979	0.00021	0.00000	0.10215		**722**	0.99672	0.00328	0.00000	0.10215
	321	0.57589	0.42408	0.00003	0.10215		**723**	0.99999	0.00001	0.00000	0.10215
	322	0.00000	0.99871	0.00129	1		**724**	0.99995	0.00005	0.00000	0.10215
	323	1	0.00000	0.00000	0.10215		**725**	0.14109	0.85708	0.00182	1
	324	0.99996	0.00004	0.00000	0.10215		**726**	0.99992	0.00008	0.00000	0.10215
	325	0.00048	0.99482	0.00469	1		**727**	0.99992	0.00008	0.00000	0.10215
	326	0.00020	0.99771	0.00208	1		**728**	0.00000	0.92280	0.07720	1
	327	0.99974	0.00026	0.00000	0.10215		**729**	0.80969	0.19029	0.00002	0.10215
	328	0.99493	0.00507	0.00000	0.10215		**730**	0.99987	0.00013	0.00000	0.10215
	329	0.00000	0.79026	0.20974	1		**731**	0.99347	0.00653	0.00000	0.10215
	330	0.99722	0.00278	0.00000	0.10215		**732**	0.00000	0.00002	0.99998	2,56612
	331	0.99873	0.00127	0.00000	0.10215		**733**	0.80017	0.19981	0.00002	0.10215
	332	0.99996	0.00004	0.00000	0.10215		**734**	0.99768	0.00232	0.00000	0.10215
	333	0.99649	0.00351	0.00000	0.10215		**735**	0.49928	0.50066	0.00006	1
	334	0.99809	0.00191	0.00000	0.10215		**736**	0.00068	0.99645	0.00287	1
	335	0.97910	0.02090	0.00000	0.10215		**737**	0.34226	0.65754	0.00020	1
	336	0.99908	0.00092	0.00000	0.10215		**738**	0.98428	0.01572	0.00000	0.10215
	337	0.00000	0.97049	0.02950	1		**739**	0.31005	0.68990	0.00005	1

	338	0.99455	0.00545	0.00000	0.10215		**740**	0.03702	0.96268	0.00030	1
	339	0.00067	0.99792	0.00141	1	*Transmembrane*	**741**	0.42008	0.57992	0.00000	1
	340	0.04261	0.95509	0.00231	1		**742**	0.99493	0.00507	0.00000	0.10215
	341	0.99941	0.00059	0.00000	0.10215		**743**	0.99666	0.00334	0.00000	0.10215
	342	0.99942	0.00058	0.00000	0.10215		**744**	0.99993	0.00007	0.00000	0.10215
	343	0.66924	0.33074	0.00002	0.10215		**745**	0.00600	0.99385	0.00015	1
	344	0.99893	0.00107	0.00000	0.10215		**746**	0.99995	0.00005	0.00000	0.10215
	345	0.99990	0.00010	0.00000	0.10215		**747**	0.99988	0.00012	0.00000	0.10215
	346	0.99871	0.00129	0.00000	0.10215		**748**	0.97979	0.02021	0.00000	0.10215
	347	0.99986	0.00014	0.00000	0.10215		**749**	0.99991	0.00009	0.00000	0.10215
	348	0.99995	0.00005	0.00000	0.10215		**750**	0.99999	0.00001	0.00000	0.10215
	349	0.99493	0.00507	0.00000	0.10215		**751**	0.70157	0.29842	0.00001	0.10215
	350	0.99999	0.00001	0.00000	0.10215		**752**	0.00000	0.30667	0.69333	2,56612
	351	0.98076	0.01924	0.00000	0.10215		**753**	0.83656	0.16344	0.00000	0.10215
	352	0.99467	0.00533	0.00000	0.10215		**754**	0.99572	0.00428	0.00000	0.10215
	353	0.84511	0.15489	0.00000	0.10215		**755**	0.00730	0.99261	0.00010	1
	354	0.00000	0.67987	0.32013	1		**756**	0.99388	0.00612	0.00000	0.10215
	355	0.99999	0.00001	0.00000	0.10215		**757**	0.99440	0.00560	0.00000	0.10215

	356	0.99974	0.00026	0.00000	0.10215		**758**	0.00002	0.99016	0.00982	1
	357	0.99994	0.00006	0.00000	0.10215		**759**	0.00001	0.96428	0.03572	1
	358	0.99992	0.00008	0.00000	0.10215		**760**	0.99820	0.00180	0.00000	0.10215
	359	0.14690	0.85308	0.00002	1		**761**	0.97386	0.02614	0.00000	0.10215
	360	1	0.00000	0.00000	0.10215		**762**	0.00001	0.97530	0.02469	1
	361	0.99893	0.00107	0.00000	0.10215		**763**	0.01392	0.98590	0.00018	1
	362	0.99986	0.00014	0.00000	0.10215		**764**	0.99988	0.00012	0.00000	0.10215
	363	0.99999	0.00001	0.00000	0.10215		**765**	0.99992	0.00008	0.00000	0.10215
	364	0.99542	0.00458	0.00000	0.10215		**766**	0.97316	0.02684	0.00000	0.10215
	365	0.99913	0.00087	0.00000	0.10215		**767**	0.00000	0.99921	0.00079	1
	366	1	0.00000	0.00000	0.10215		**768**	0.96403	0.03596	0.00001	0.10215
	367	0.99808	0.00192	0.00000	0.10215		**769**	0.18348	0.81650	0.00001	1
	368	0.96687	0.03313	0.00000	0.10215		**770**	0.99214	0.00786	0.00000	0.10215
	369	0.99974	0.00026	0.00000	0.10215		**771**	0.42629	0.57371	0.00000	1
	370	0.99683	0.00317	0.00000	0.10215		**772**	0.00000	0.99150	0.00850	1
	371	0.99987	0.00013	0.00000	0.10215		**773**	0.02291	0.97637	0.00072	1
	372	0.99981	0.00019	0.00000	0.10215		**774**	0.00002	0.98365	0.01633	1
	373	0.99998	0.00002	0.00000	0.10215		**775**	0.00001	0.99189	0.00810	1

	374	0.99996	0.00004	0.00000	0.10215		**776**	0.00011	0.99922	0.00068	1
	375	0.99999	0.00001	0.00000	0.10215		**777**	0.99934	0.00066	0.00000	0.10215
	376	1	0.00000	0.00000	0.10215		**778**	0.99942	0.00058	0.00000	0.10215
	377	0.99982	0.00018	0.00000	0.10215		**779**	1	0.00000	0.00000	0.10215
	378	0.99990	0.00010	0.00000	0.10215		**780**	0.99966	0.00034	0.00000	0.10215
	379	0.99993	0.00007	0.00000	0.10215		**781**	0.99989	0.00011	0.00000	0.10215
	380	0.99945	0.00055	0.00000	0.10215		**782**	0.04027	0.95947	0.00027	1
	381	0.99991	0.00009	0.00000	0.10215		**783**	0.10549	0.89407	0.00043	1
	382	0.99964	0.00036	0.00000	0.10215		**784**	0.01323	0.98658	0.00019	1
	383	1	0.00000	0.00000	0.10215		**785**	0.98593	0.01407	0.00000	0.10215
	384	0.99987	0.00013	0.00000	0.10215		**786**	0.00011	0.99259	0.00730	1
	385	0.99991	0.00009	0.00000	0.10215		**787**	0.00019	0.99957	0.00023	1
	386	0.99860	0.00140	0.00000	0.10215		**788**	0.97281	0.02719	0.00000	0.10215
	387	0.00000	0.00006	0.99994	2,56612		**789**	0.99087	0.00913	0.00000	0.10215
	388	0.99937	0.00063	0.00000	0.10215		**790**	0.99992	0.00008	0.00000	0.10215
	389	0.99471	0.00529	0.00000	0.10215		**791**	0.06876	0.93124	0.00000	1
	390	0.17172	0.82814	0.00014	1		**792**	0.99999	0.00001	0.00000	0.10215
	391	0.99664	0.00336	0.00000	0.10215		**793**	0.00023	0.98351	0.01627	1

	392	0.86944	0.13051	0.00005	0.10215		**794**	0.90080	0.09920	0.00000	0.10215
	393	0.99923	0.00077	0.00000	0.10215		**795**	0.98817	0.01183	0.00000	0.10215
	394	0.45296	0.54704	0.00000	1		**796**	0.97189	0.02811	0.00000	0.10215
	395	0.99981	0.00019	0.00000	0.10215		**797**	0.20042	0.79957	0.00000	1
	396	0.99995	0.00005	0.00000	0.10215		**798**	0.00000	0.14867	0.85133	2,56612
	397	1	0.00000	0.00000	0.10215		**799**	0.99646	0.00354	0.00000	0.10215
	398	0.99999	0.00001	0.00000	0.10215		**800**	0.99992	0.00008	0.00000	0.10215
	399	0.99990	0.00010	0.00000	0.10215		**801**	0.00013	0.99892	0.00096	1
	400	0.99977	0.00023	0.00000	0.10215		**802**	0.99944	0.00056	0.00000	0.10215
	401	0.99998	0.00002	0.00000	0.10215		**803**	0.99995	0.00005	0.00000	0.10215
	402	0.99999	0.00001	0.00000	0.10215		**804**	0.99781	0.00219	0.00000	0.10215